

**Electronic supplementary information for**

**Synthesis of 2-bromo- and 2-phenyl-neo-confused porphyrins**

Arwa S. Almejbel and Timothy D. Lash\*

Department of Chemistry, Illinois State University, Normal, Illinois 61790-4160

E-mail: [tdlash@ilstu.edu](mailto:tdlash@ilstu.edu)

**Table of Contents**

Page

2-6	Selected UV-Vis spectra (Figures S1-S8)
7-37	Selected proton, DEPT-135, $^1\text{H}$ - $^1\text{H}$ COSY, HSQC and carbon-13 NMR spectra (Figures S9-S52)
38-46	Selected EI and ESI mass spectra (Figures S53-S61)

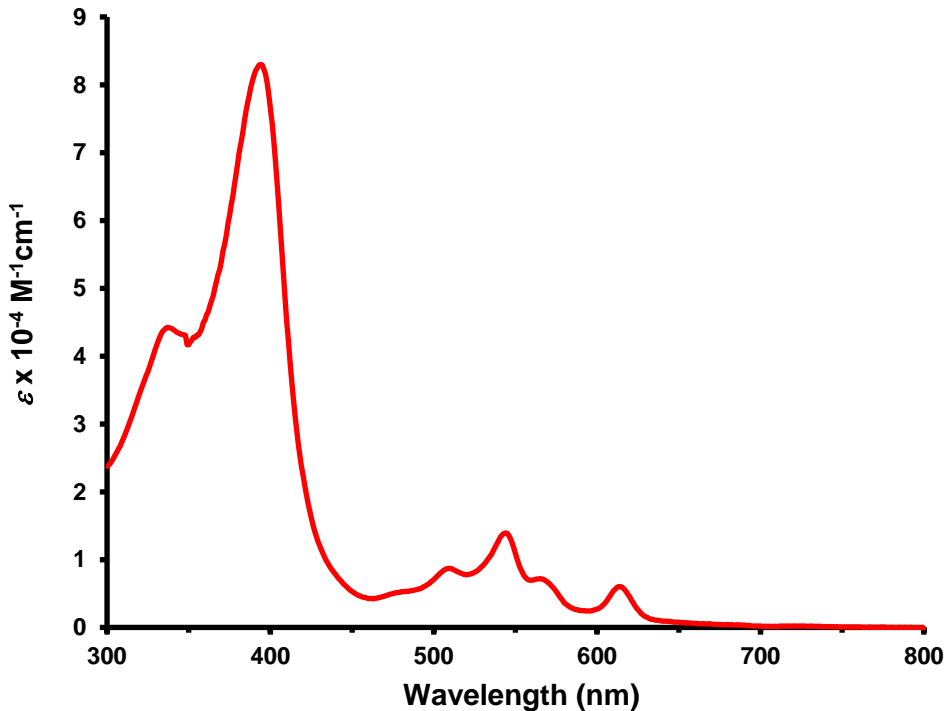


Figure S1. UV-vis spectrum of bromo-neo-confused porphyrin **8b** in 1% Et<sub>3</sub>N-chloroform.

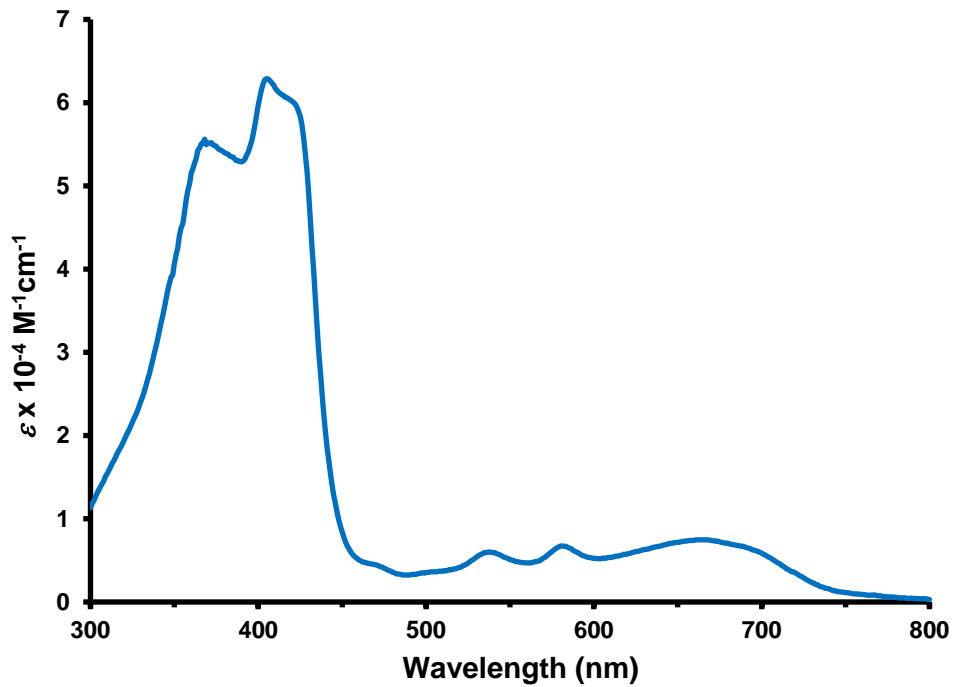


Figure S2. UV-vis spectrum of **8bH<sub>2</sub><sup>2+</sup>** in 1% TFA-CHCl<sub>3</sub>.

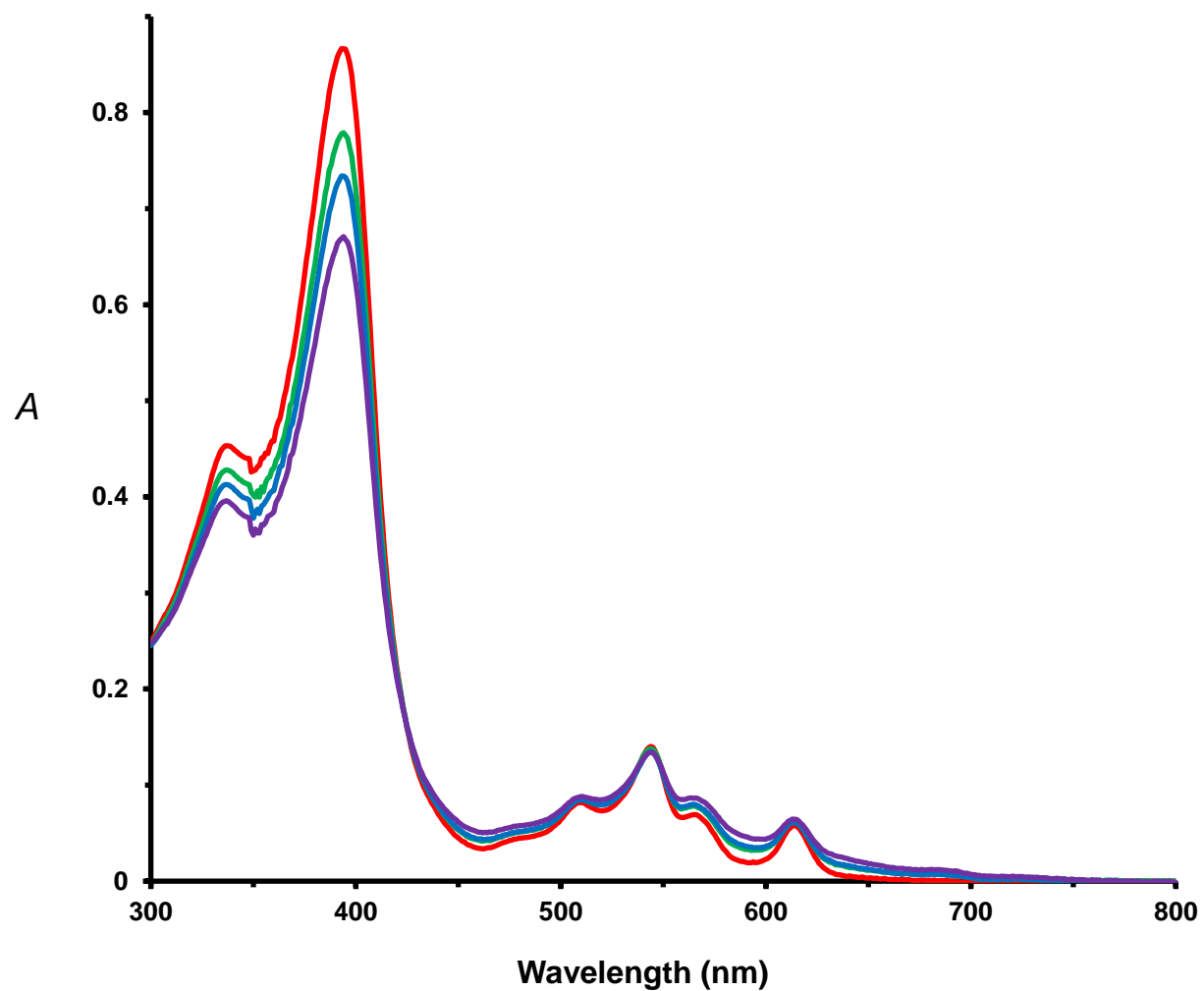


Figure S3. UV-vis spectrum of neo-confused porphyrin **8b** after 0 min (red), 30 min (green), 60 min (blue) and 120 min (purple) exposure to ambient lighting (fluorescent lights in laboratory) for a 1% Et<sub>3</sub>N-CHCl<sub>3</sub> solution in a 1 cm cuvette.

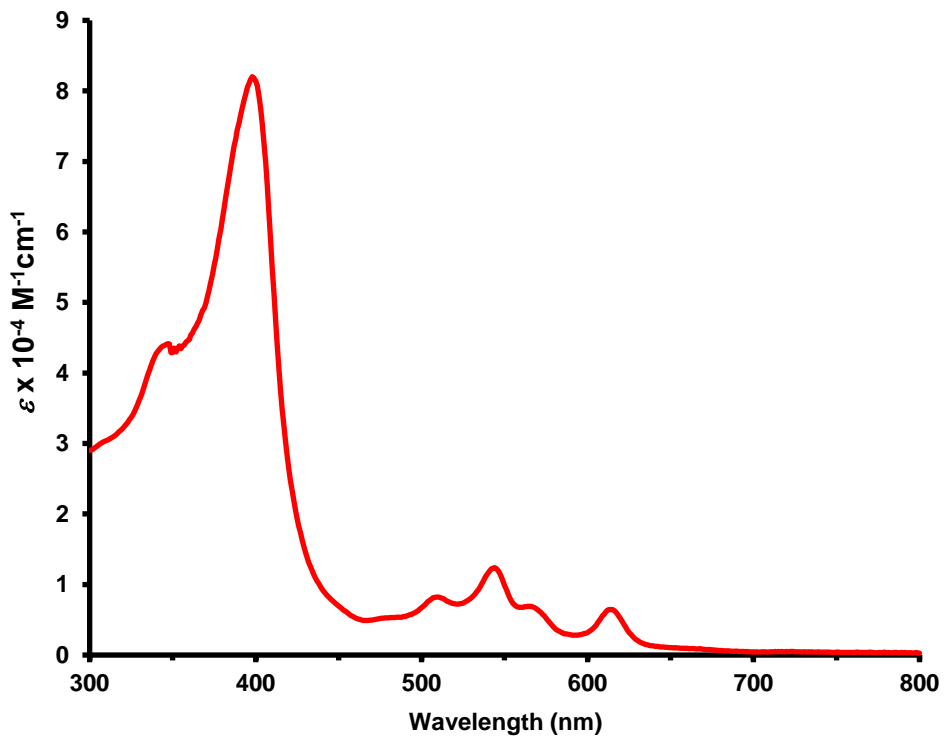


Figure S4. UV-vis spectrum of phenyl-neo-confused porphyrin **8c** in 1% Et<sub>3</sub>N-chloroform.

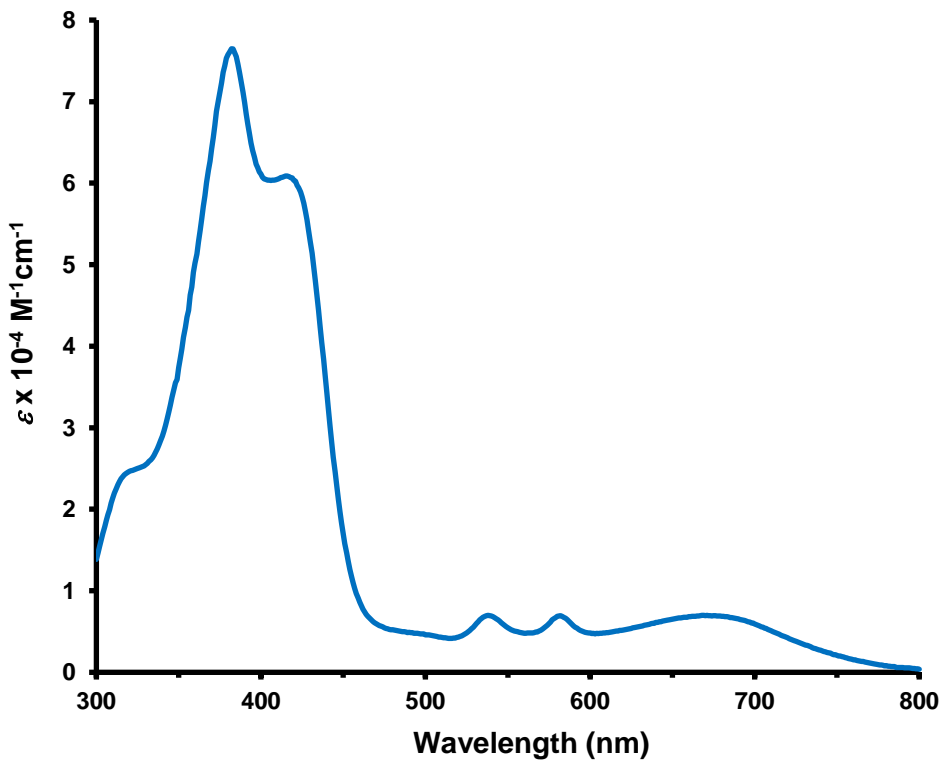


Figure S5. UV-vis spectrum of **8cH<sub>2</sub><sup>2+</sup>** in 1% TFA-chloroform.

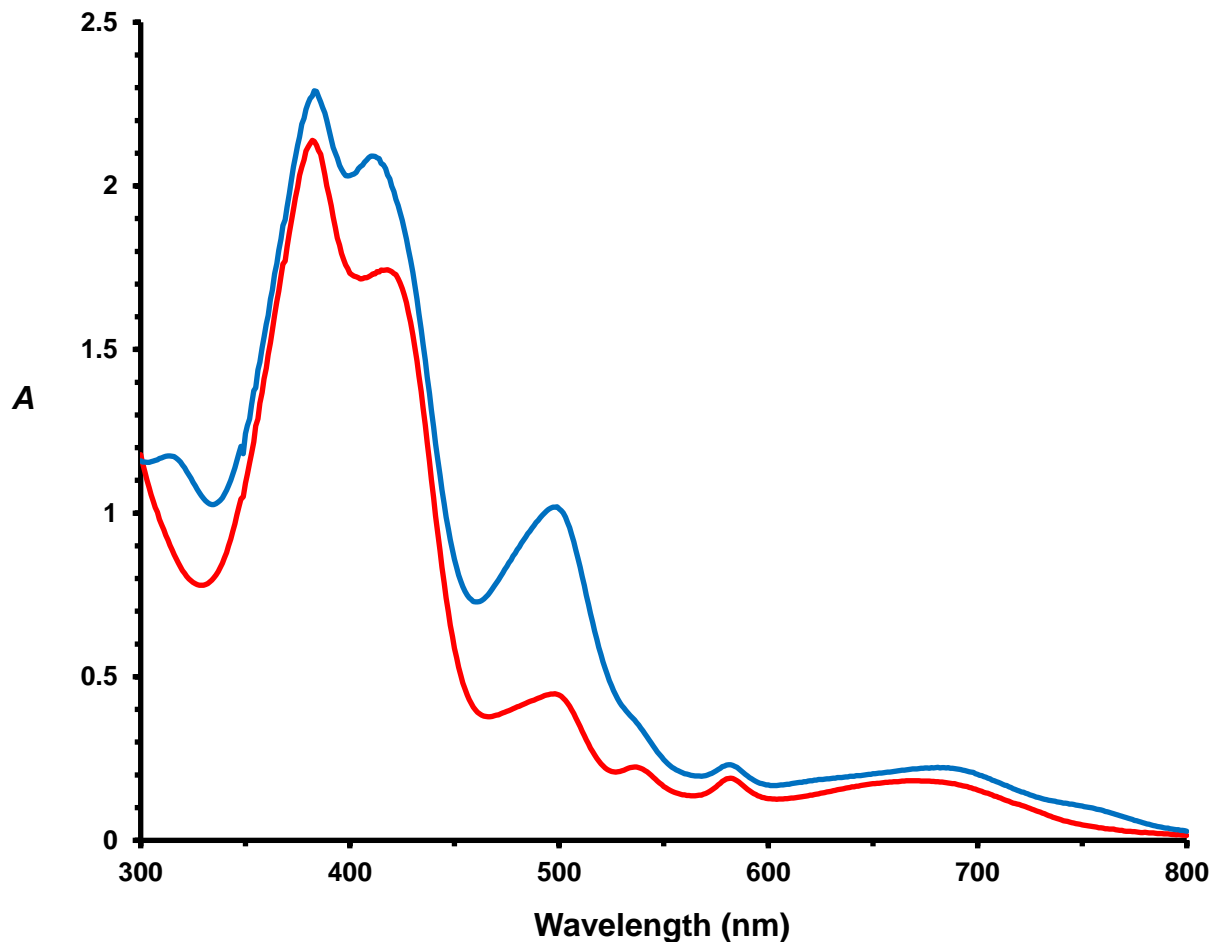


Figure S6. UV-vis spectrum of neo-confused porphyrin dication **8cH<sub>2</sub><sup>2+</sup>** after 0 min (red) and 60 min (blue) exposure to ambient lighting (fluorescent lights in laboratory) for a 1% TFA-CHCl<sub>3</sub> solution in a 1 cm cuvette. Decomposition is slower than is observed for free base neo-CP **8c**. However, the phenyl substituted neo-confused porphyrin dication is much less stable under these conditions than the related bromo-substituted species **8cH<sub>2</sub><sup>2+</sup>**.

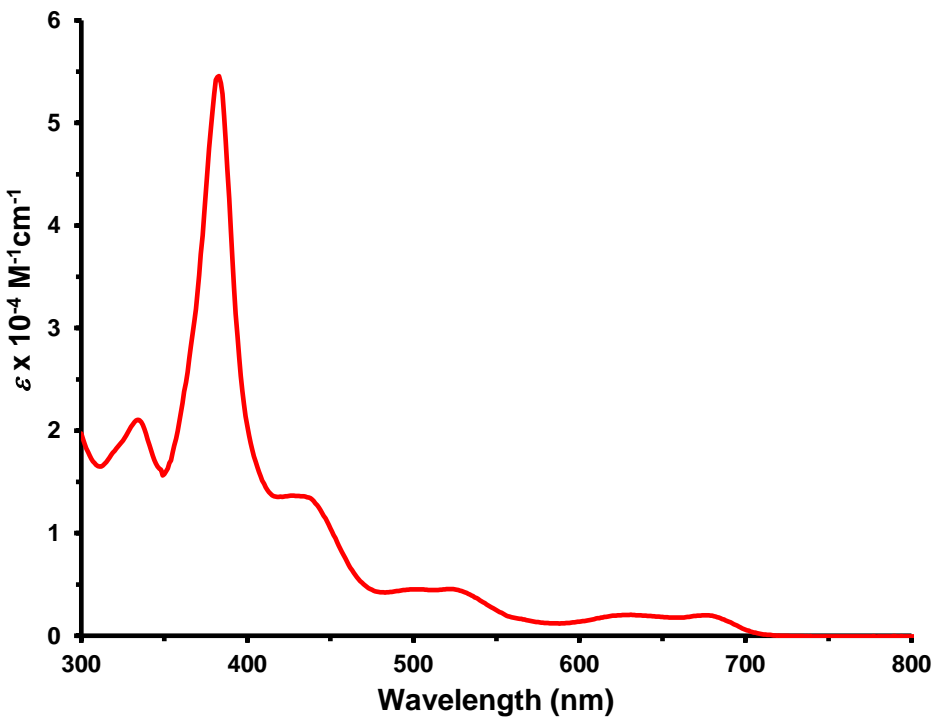


Figure S7. UV-vis spectrum of nickel(II) neo-confused porphyrin complex **18b** in chloroform.

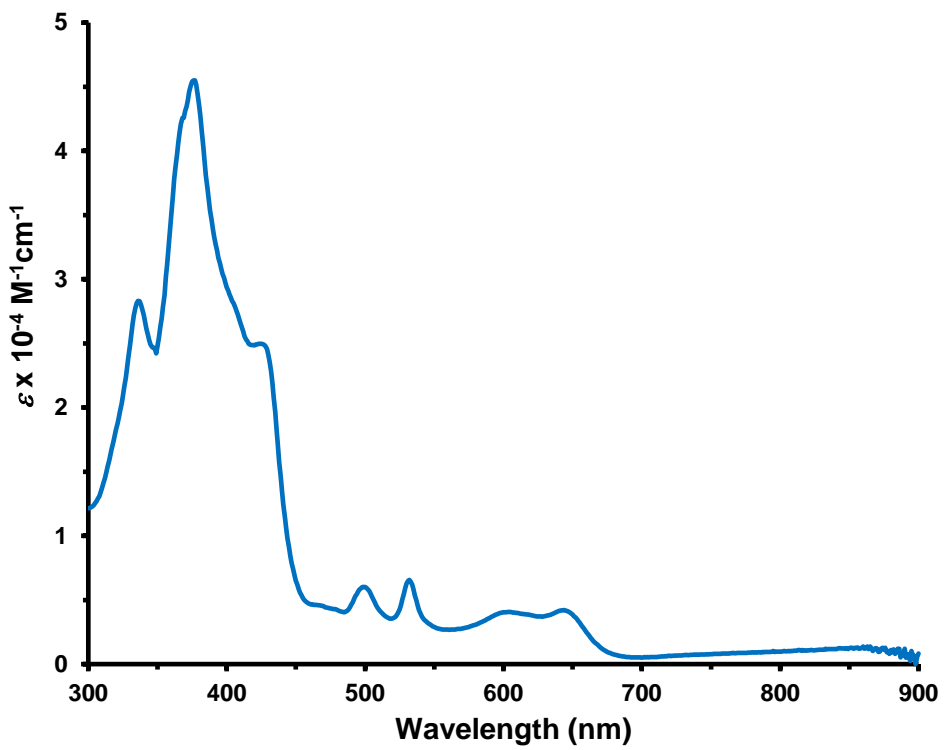


Figure S8. UV-vis spectrum of palladium(II) neo-confused porphyrin complex **19b** in chloroform.

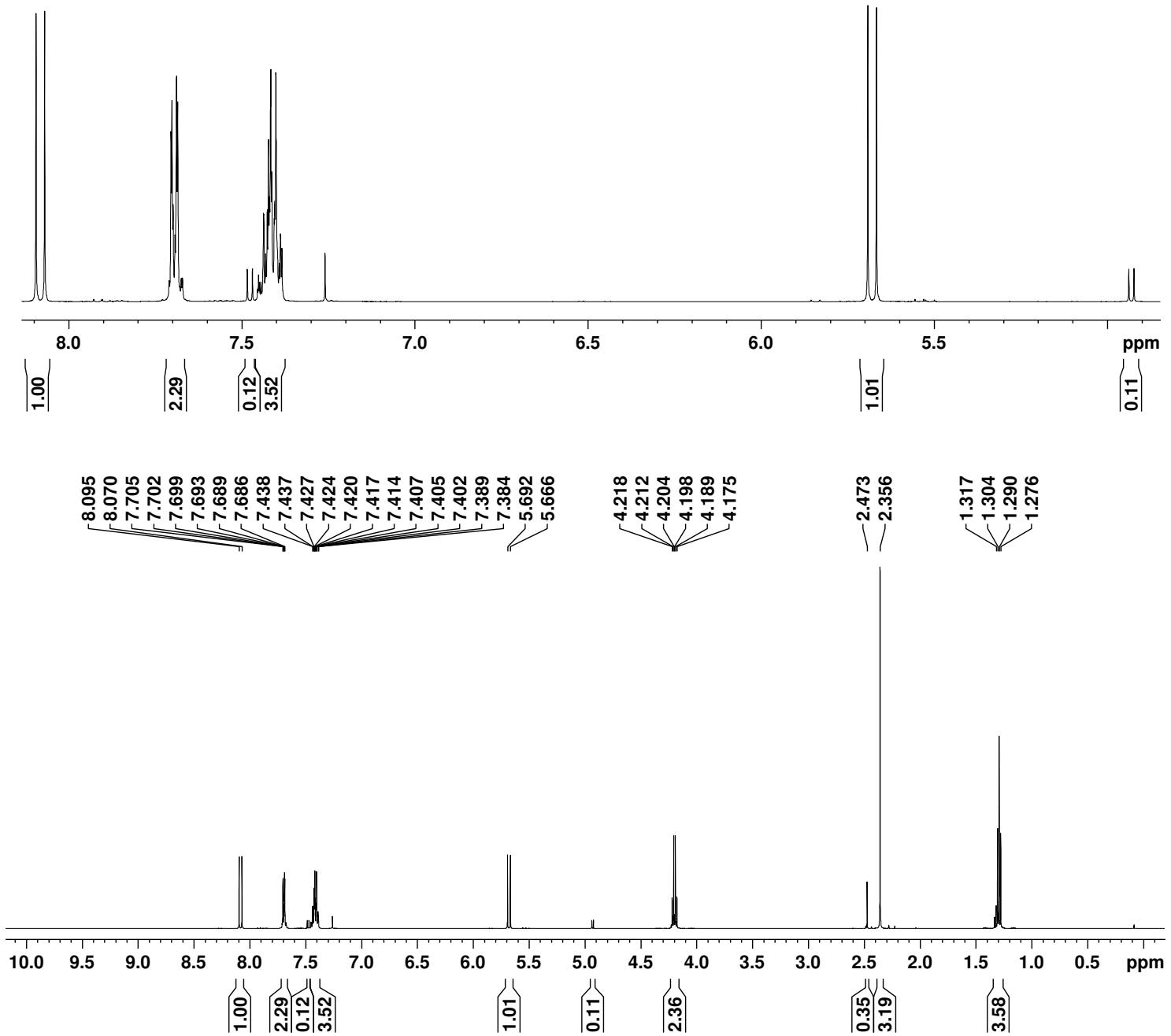


Figure S9. 500 MHz proton NMR spectrum of *E*- and *Z*-acrylates **15** (ratio 9:1) in  $\text{CDCl}_3$ .

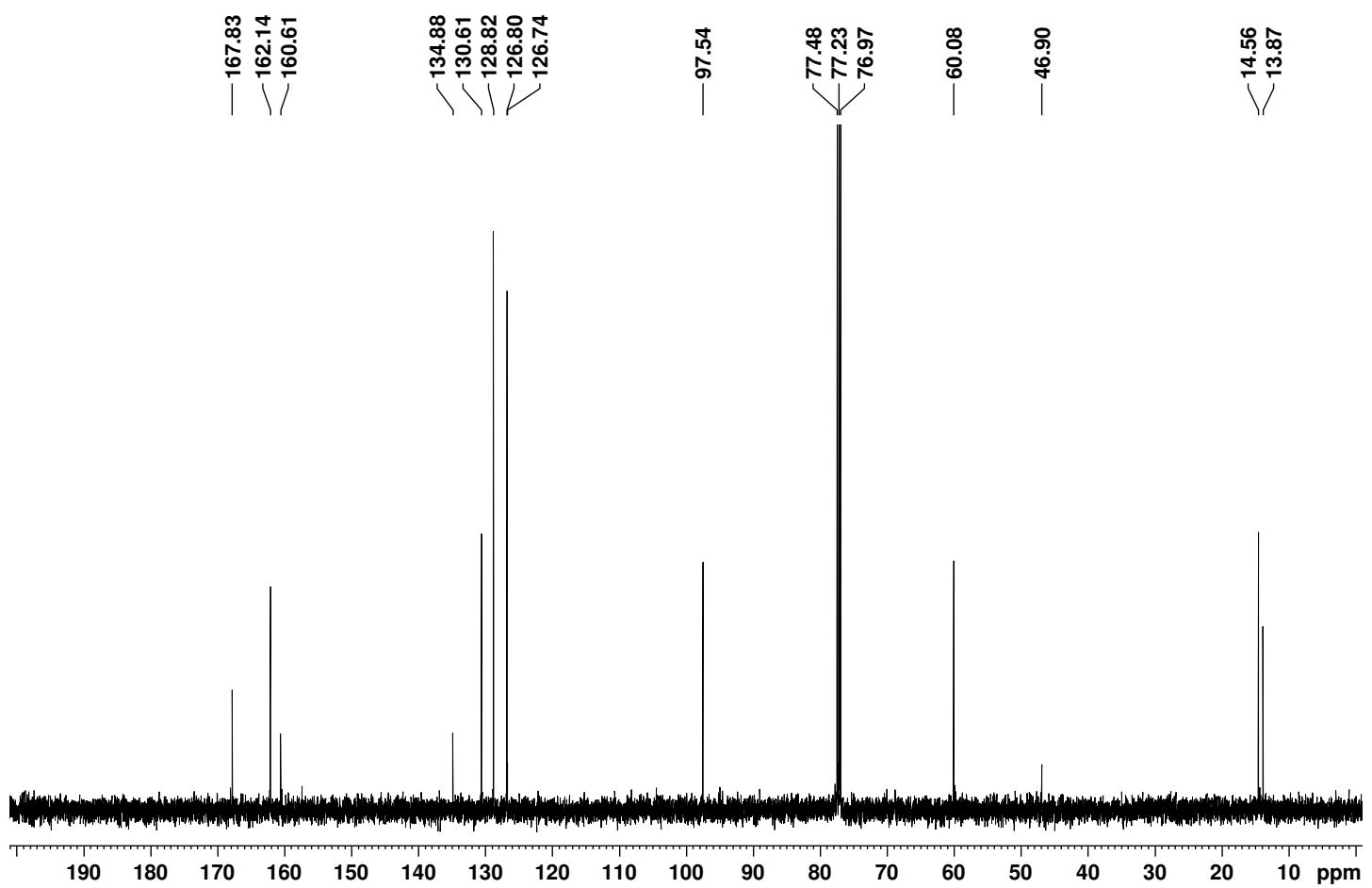


Figure S10. Carbon-13 NMR spectrum of acrylate **15** in  $\text{CDCl}_3$ .

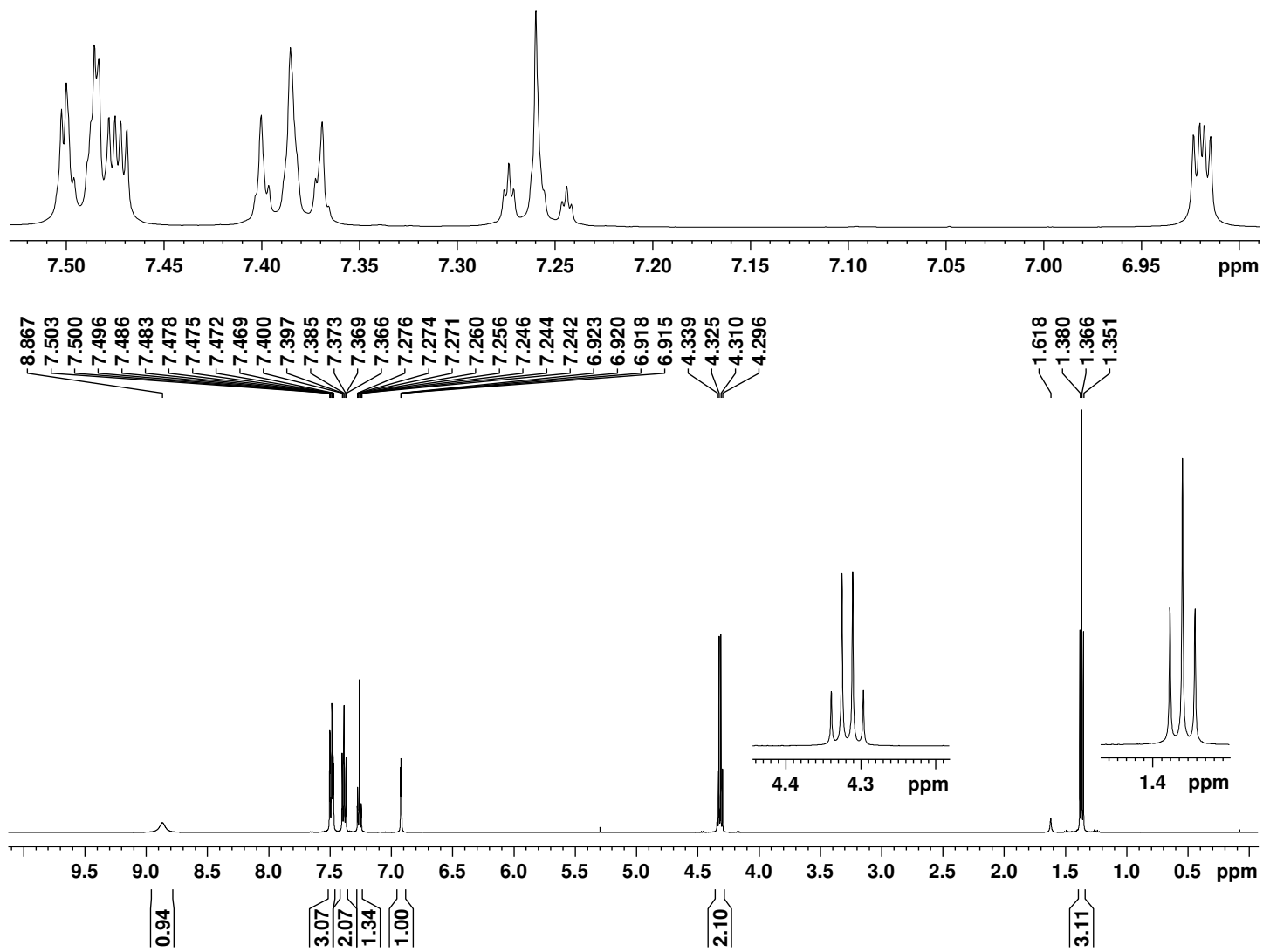


Figure S11. 500 MHz proton NMR spectrum of ethyl 5-phenylpyrrole-3-carboxylate in  $\text{CDCl}_3$ .

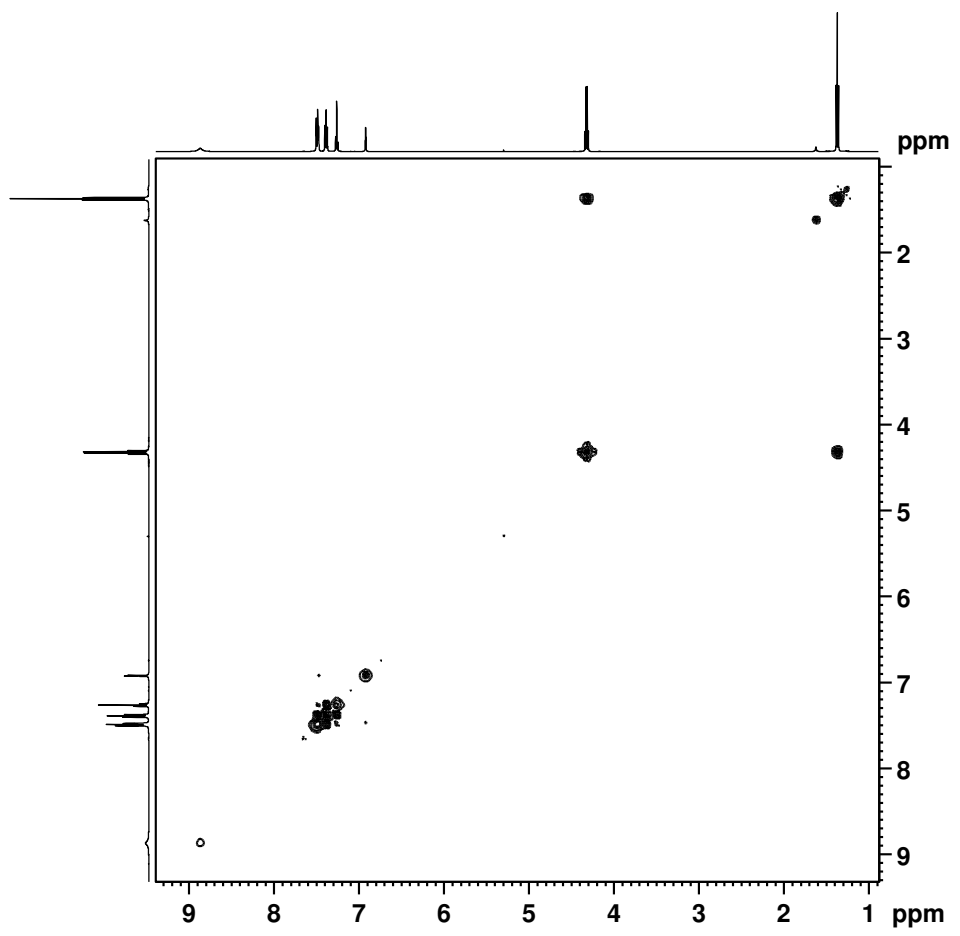


Figure S12.  $^1\text{H}$ - $^1\text{H}$  COSY NMR spectrum of ethyl 5-phenylpyrrole-3-carboxylate in  $\text{CDCl}_3$ .

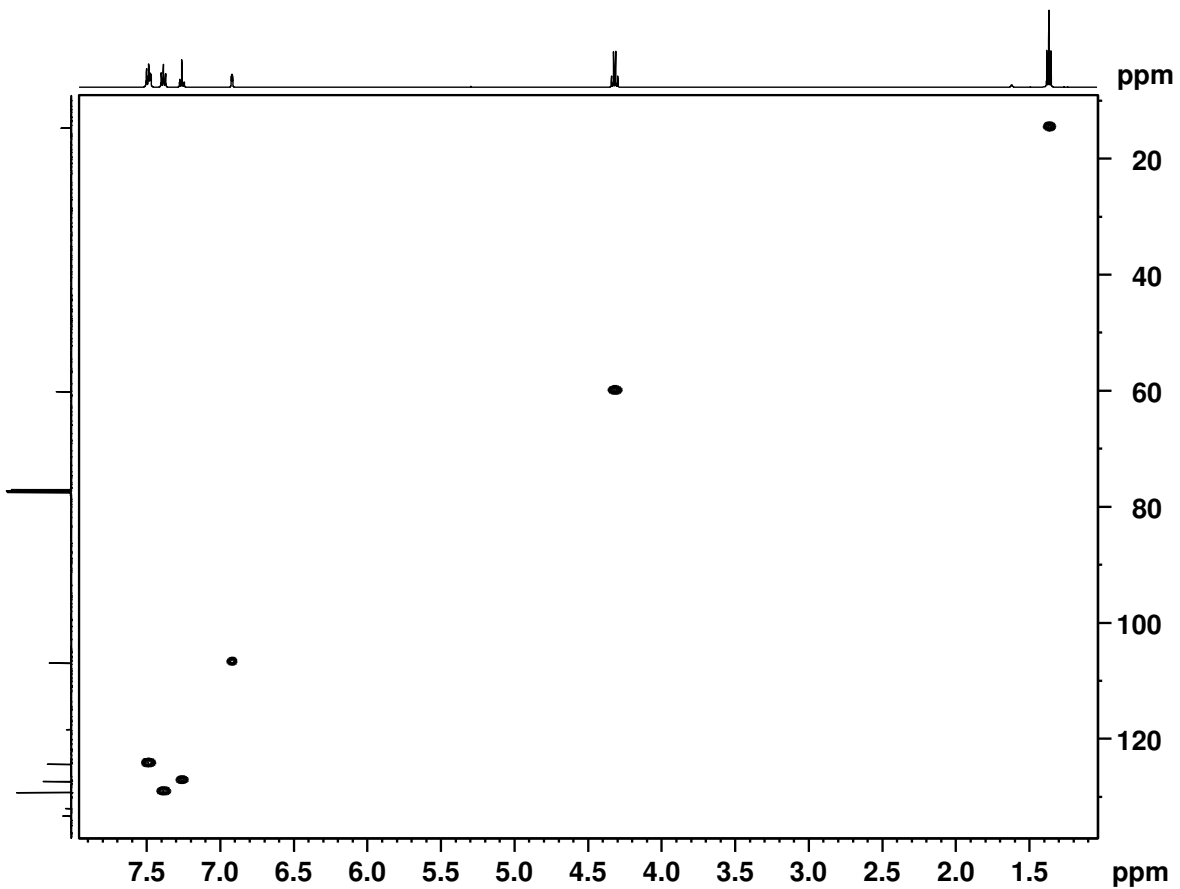


Figure S13. HSQC NMR spectrum of ethyl 5-phenylpyrrole-3-carboxylate in  $\text{CDCl}_3$ .

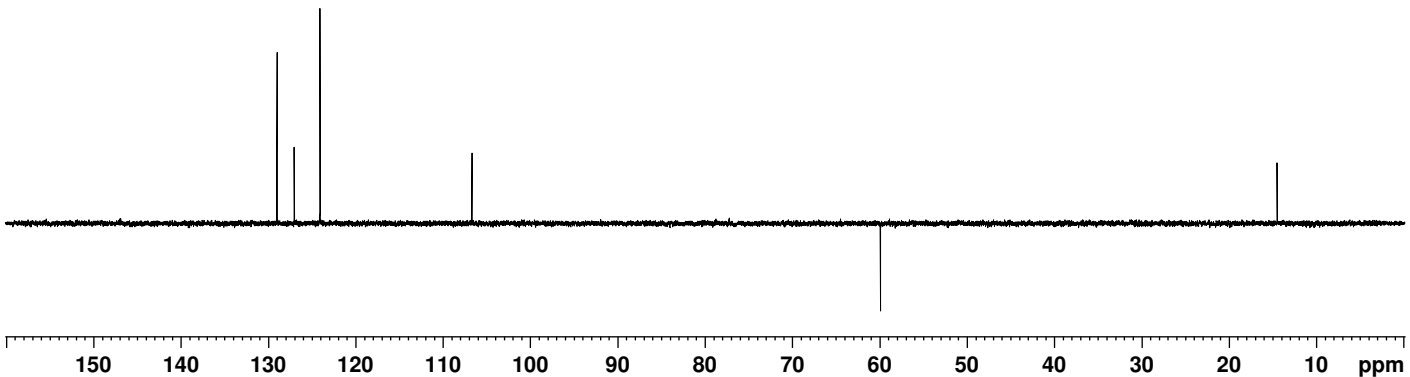


Figure S14. DEPT-135 NMR spectrum of ethyl 5-phenylpyrrole-3-carboxylate in  $\text{CDCl}_3$ .

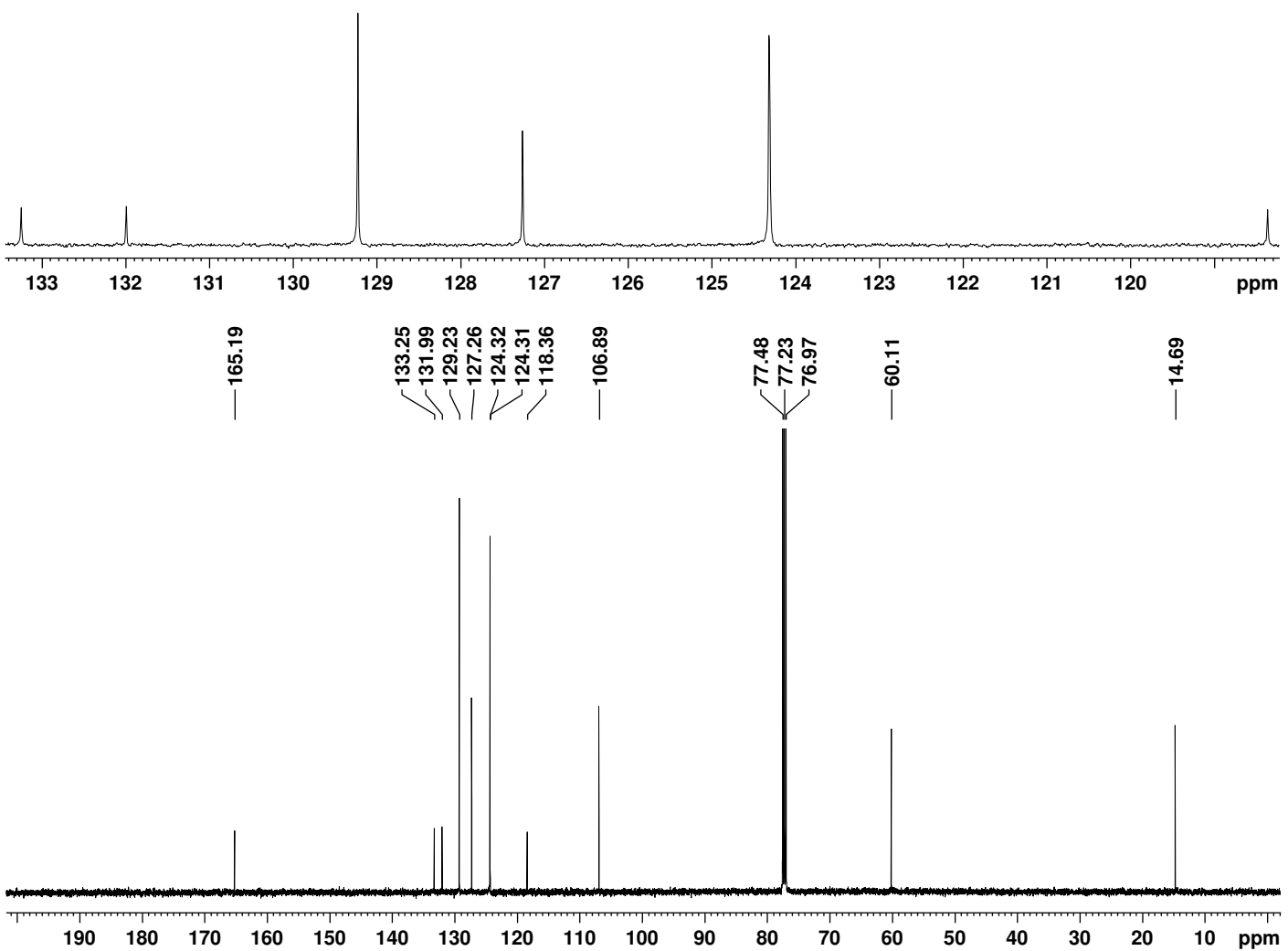


Figure S15. 125 MHz carbon-13 NMR spectrum of ethyl 5-phenylpyrrole-2-carboxylate in  $\text{CDCl}_3$ .

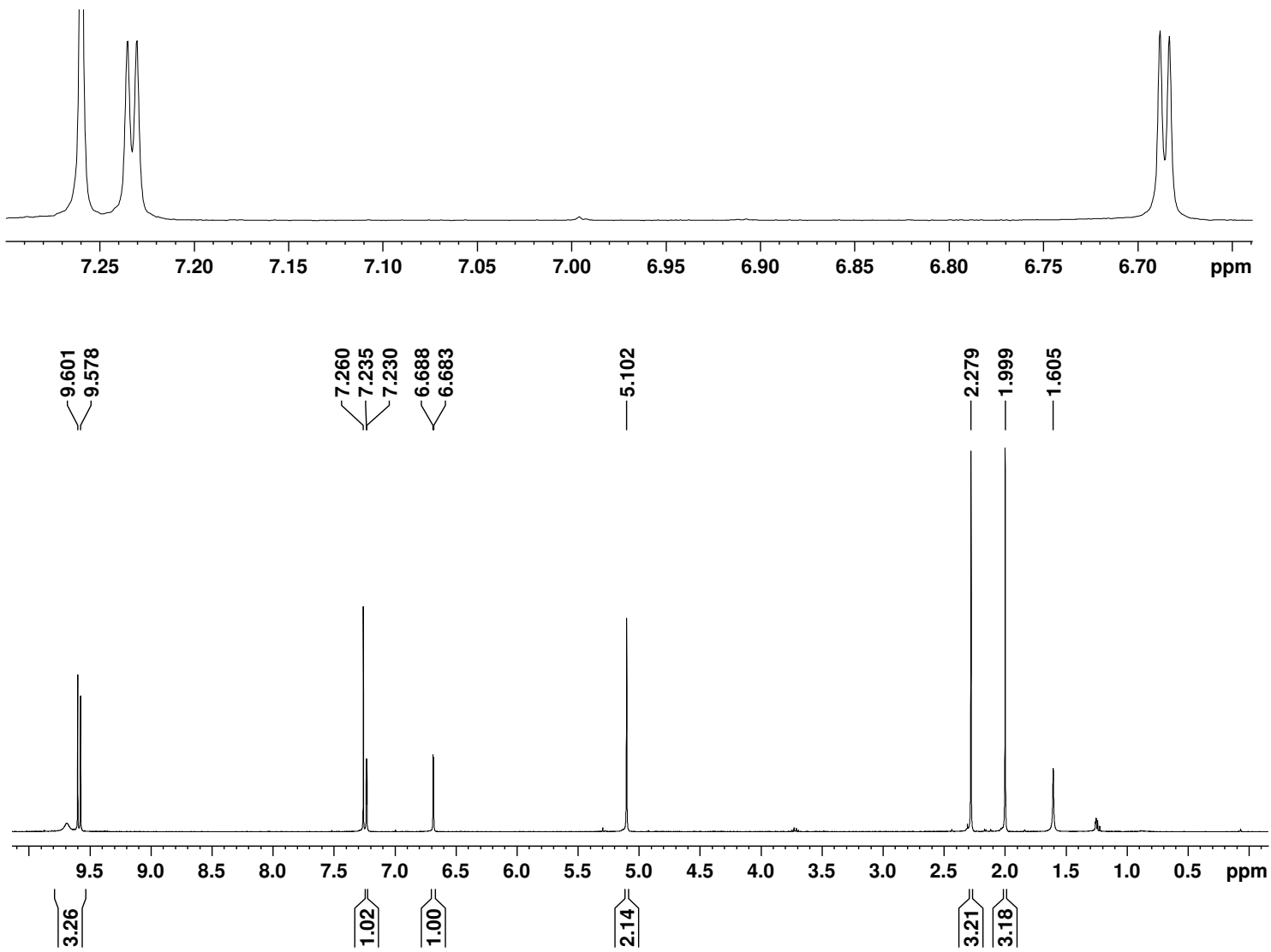


Figure S16. 500 MHz proton NMR spectrum of bromo-1,2'-dipyrrylmethane **9b** in  $\text{CDCl}_3$ .

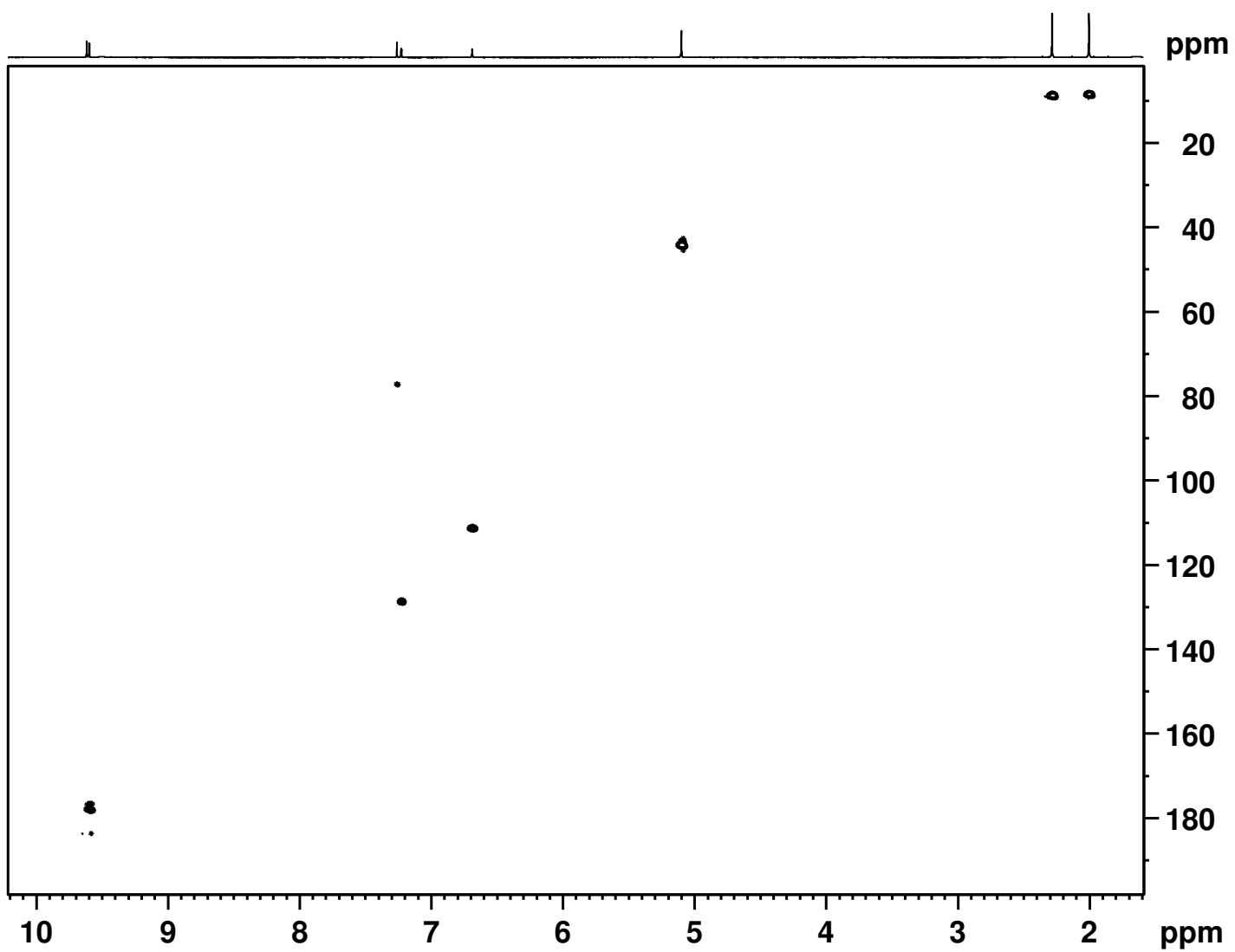


Figure S17. HSQC NMR spectrum of **9b** in  $\text{CDCl}_3$ .

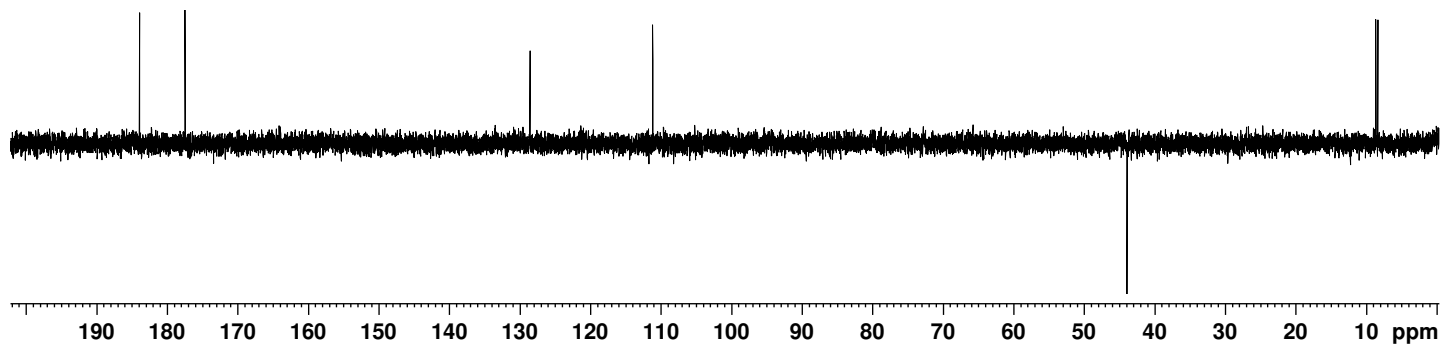


Figure S18. DEPT-135 NMR spectrum of **9b** in  $\text{CDCl}_3$ .

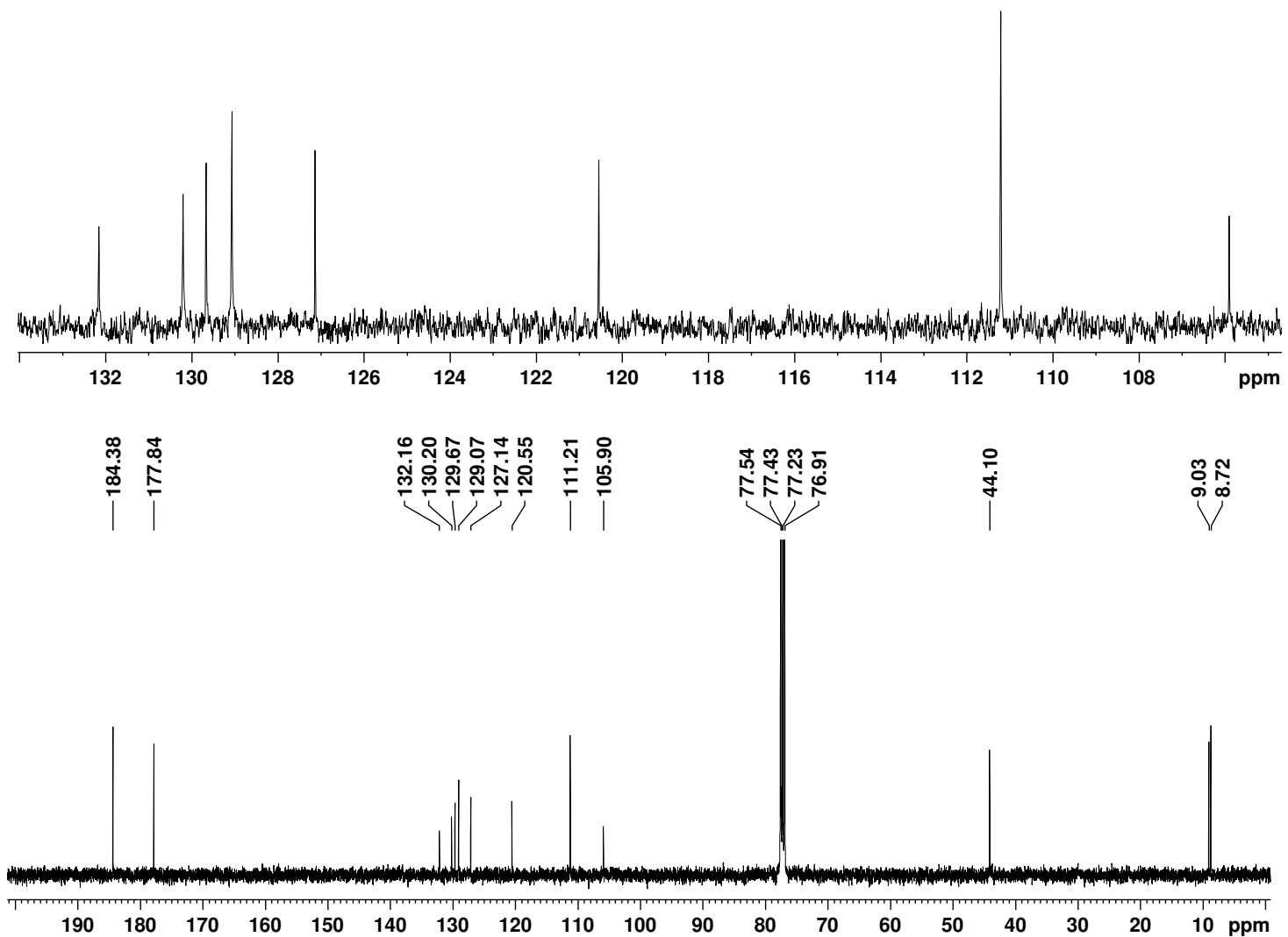


Figure S19. 125 MHz carbon-13 NMR spectrum of **9b** in  $\text{CDCl}_3$ .

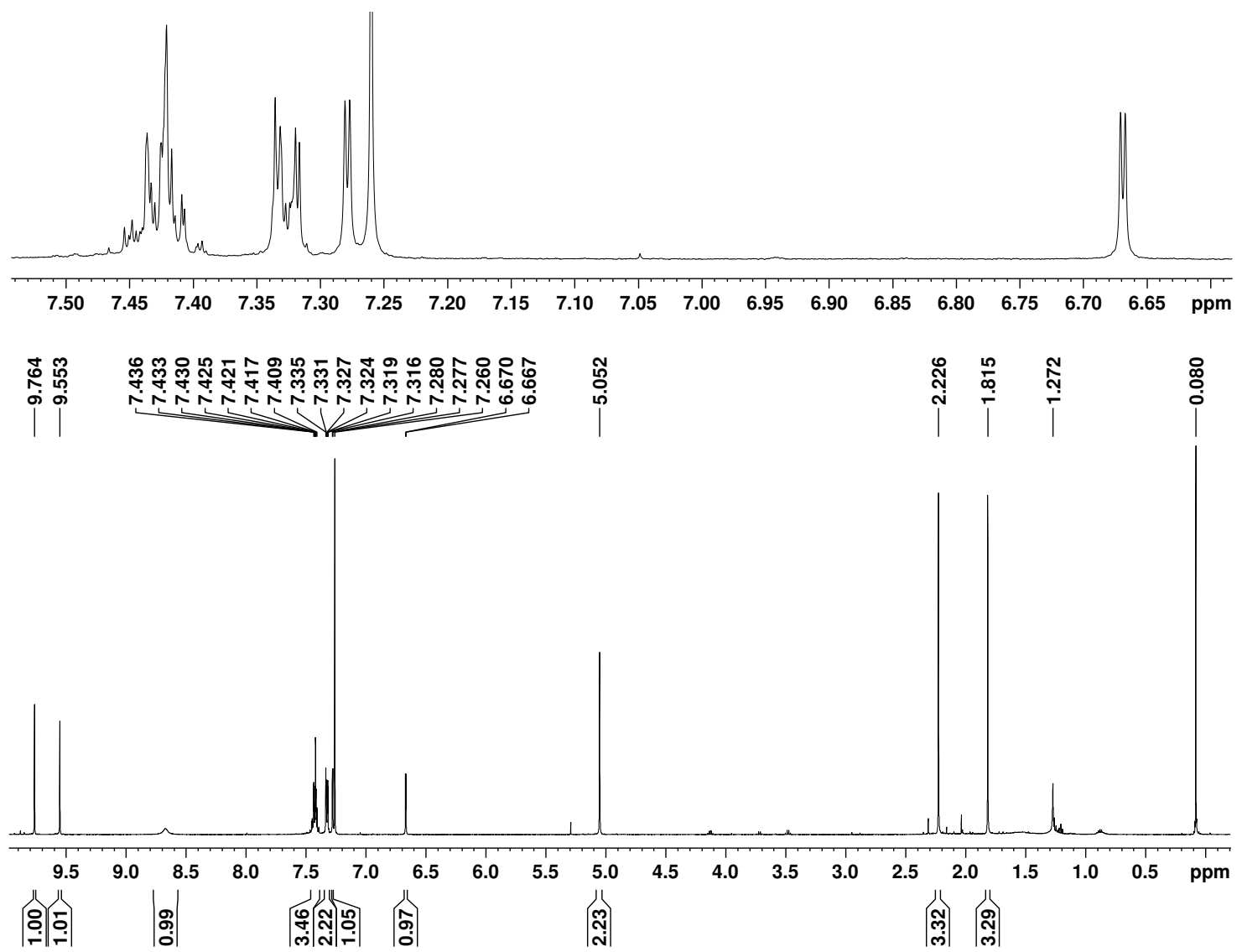


Figure S20. 500 MHz proton NMR spectrum of phenyl 1,2'-dipyrrylmethane 9c in CDCl<sub>3</sub>.

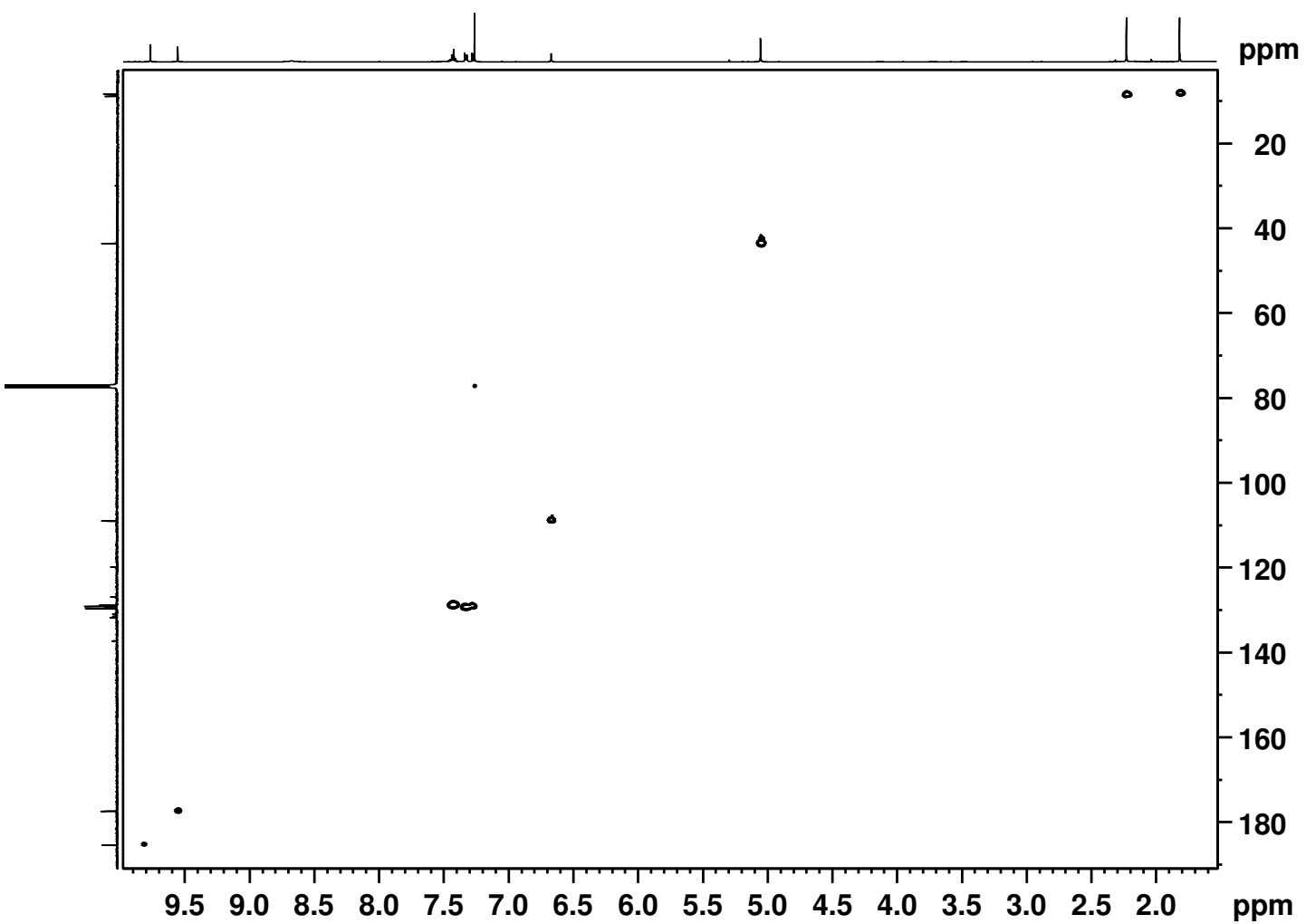


Figure S21. HSQC NMR spectrum of **9c** in  $\text{CDCl}_3$ .

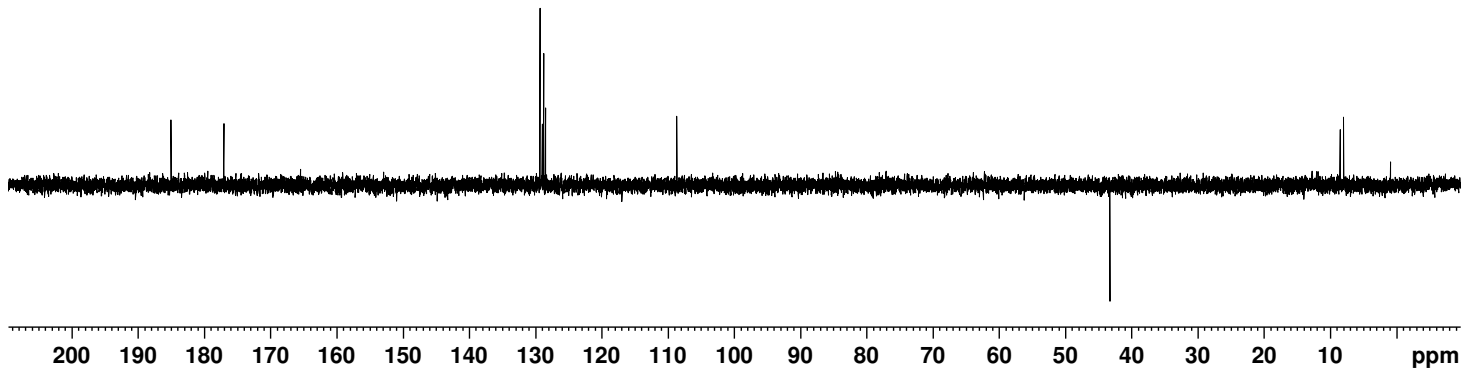


Figure S22. DEPT-135 NMR spectrum of **9c** in  $\text{CDCl}_3$ .

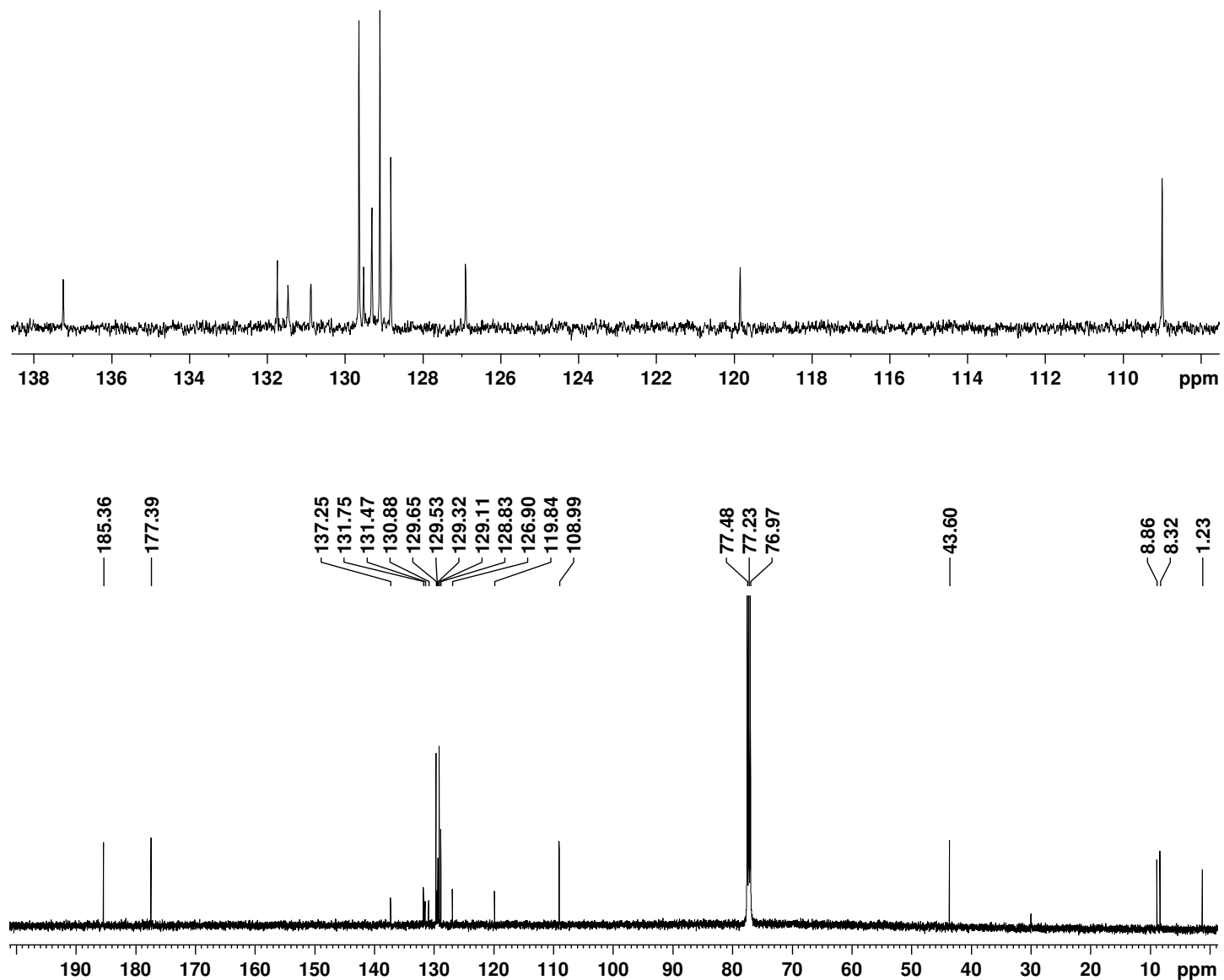


Figure S23. 125 MHz carbon-13 NMR spectrum of **9c** in  $\text{CDCl}_3$ .

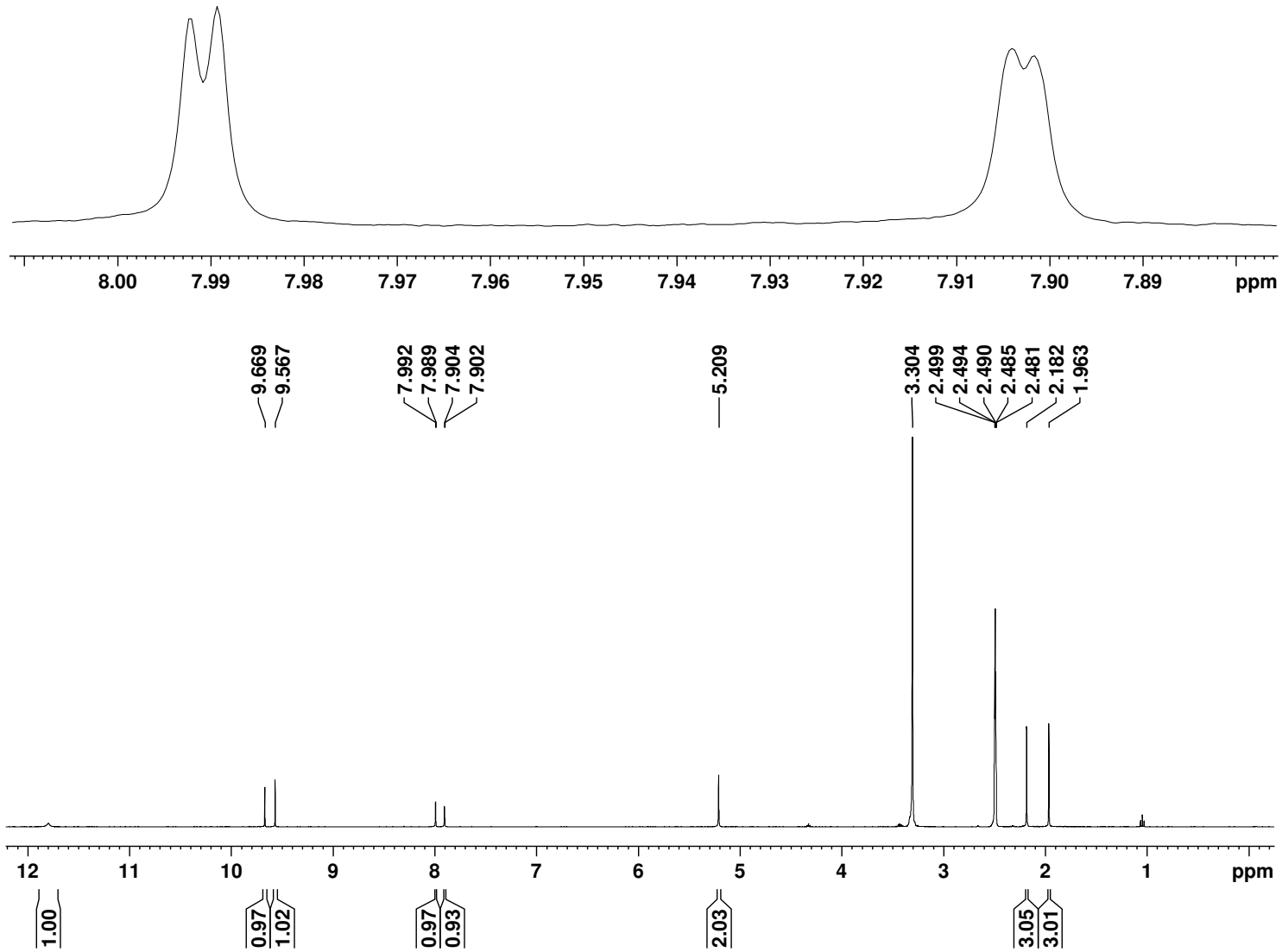


Figure S24. 500 MHz proton NMR spectrum of pyrrolylmethylimidazole **22a** in  $\text{DMSO}-d_6$ .

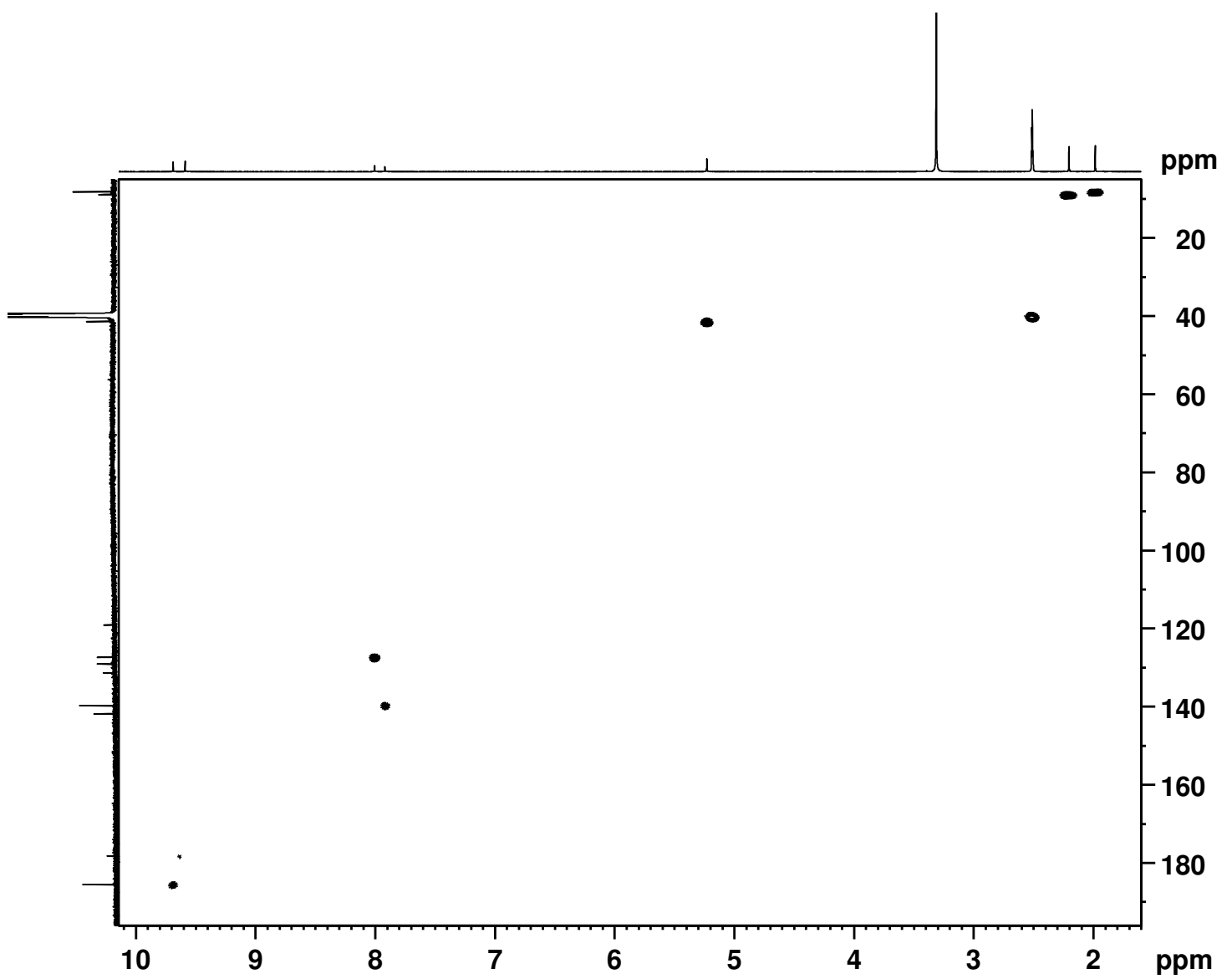


Figure S25. HSQC NMR spectrum of **22a** in  $\text{DMSO}-d_6$ .

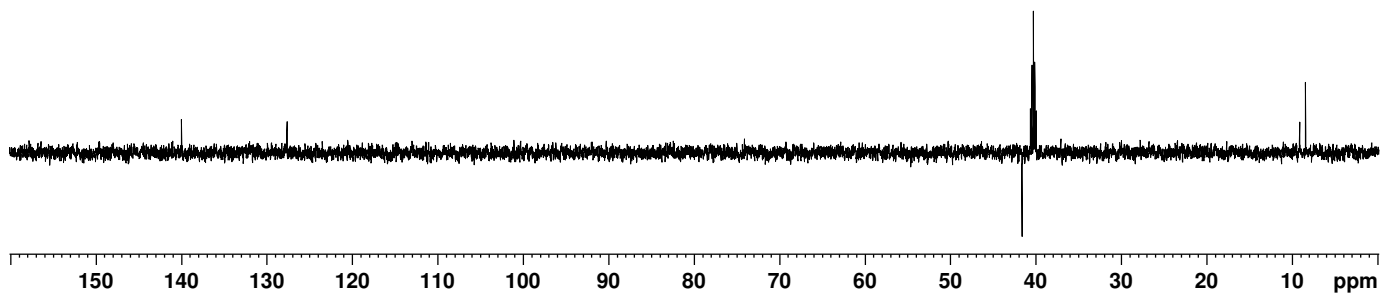


Figure S26. DEPT-135 NMR spectrum of **22a** in  $\text{DMSO}-d_6$ .

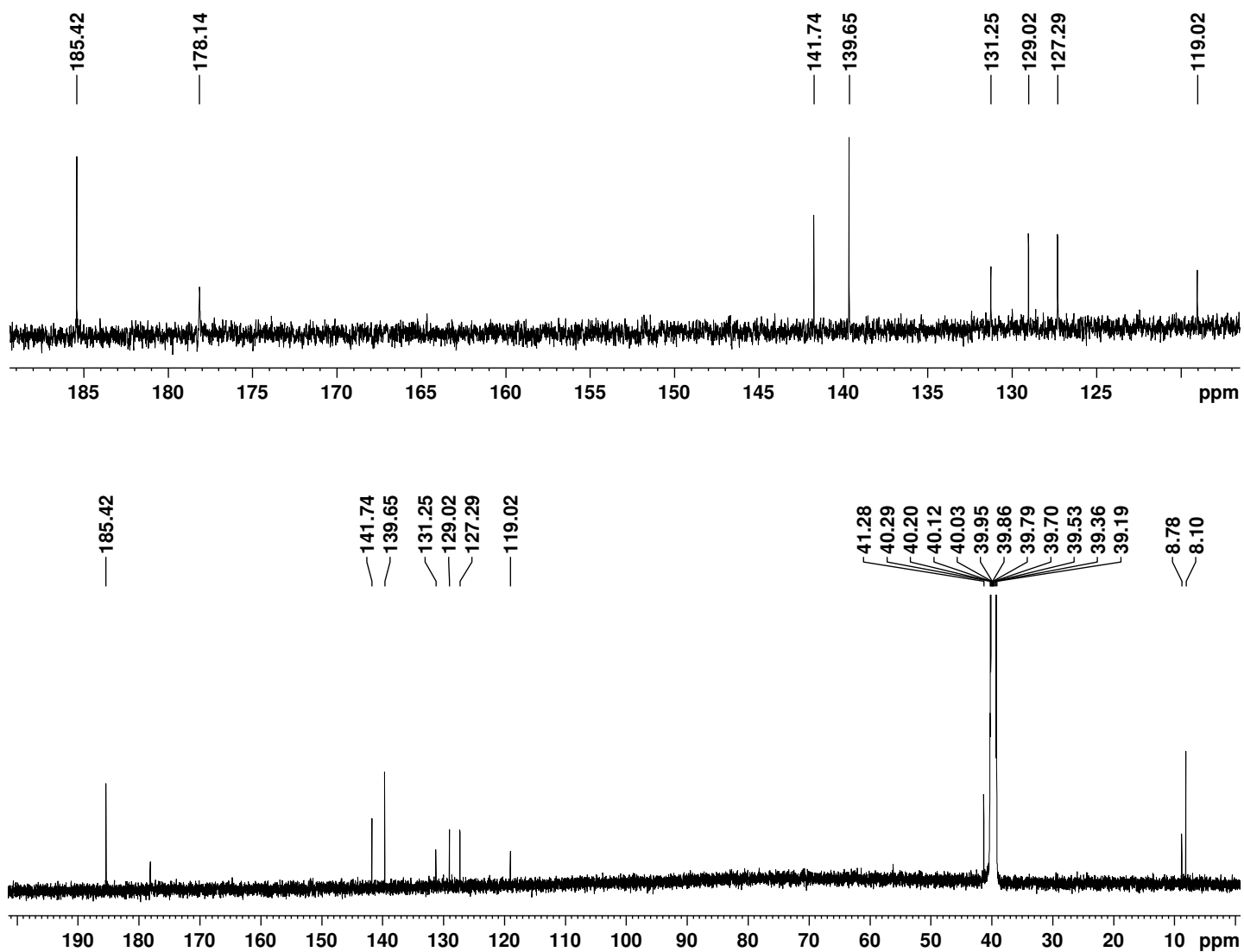
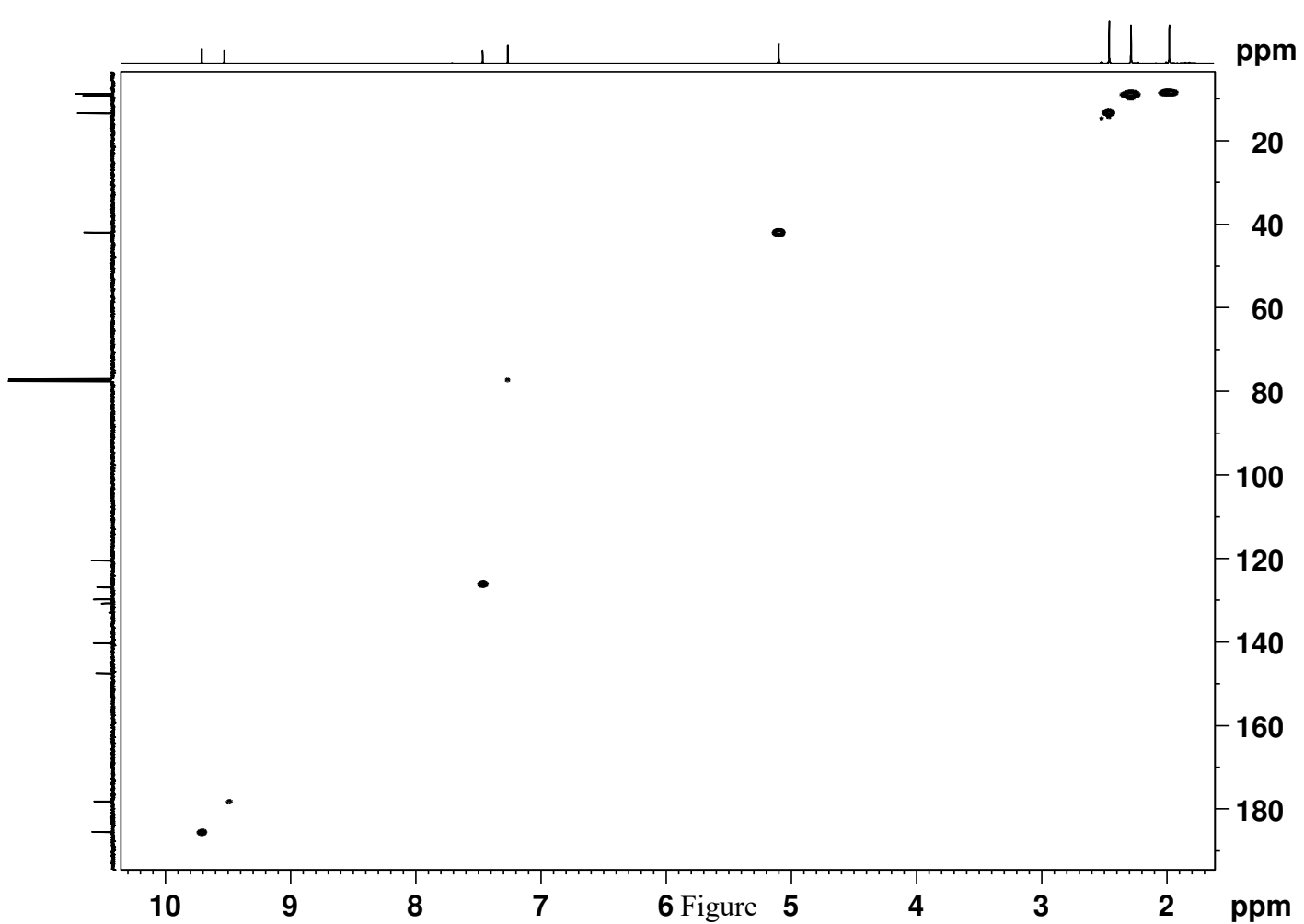
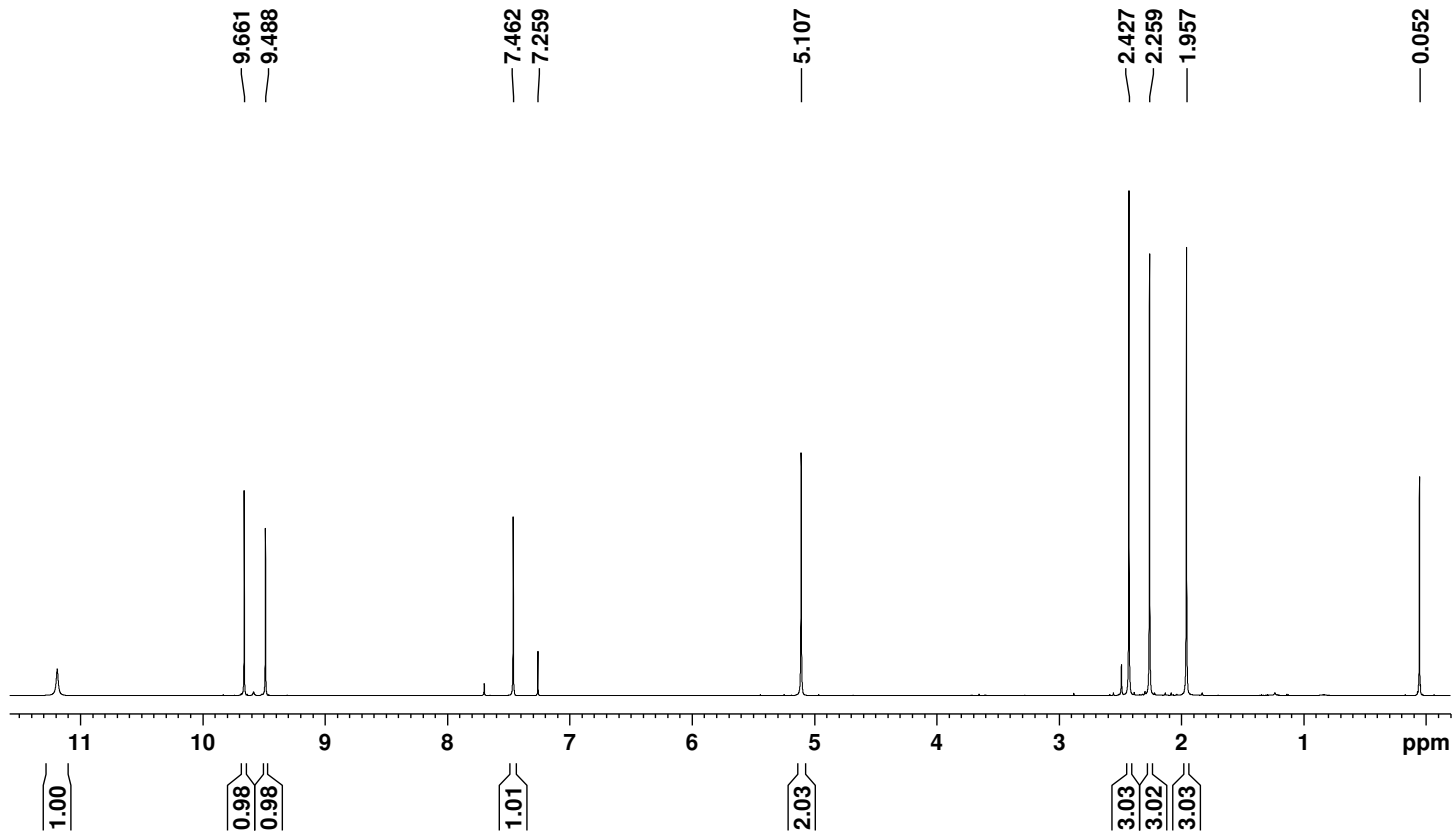


Figure S27. 125 MHz carbon-13 NMR spectrum of **22a** in  $\text{DMSO}-d_6$ .



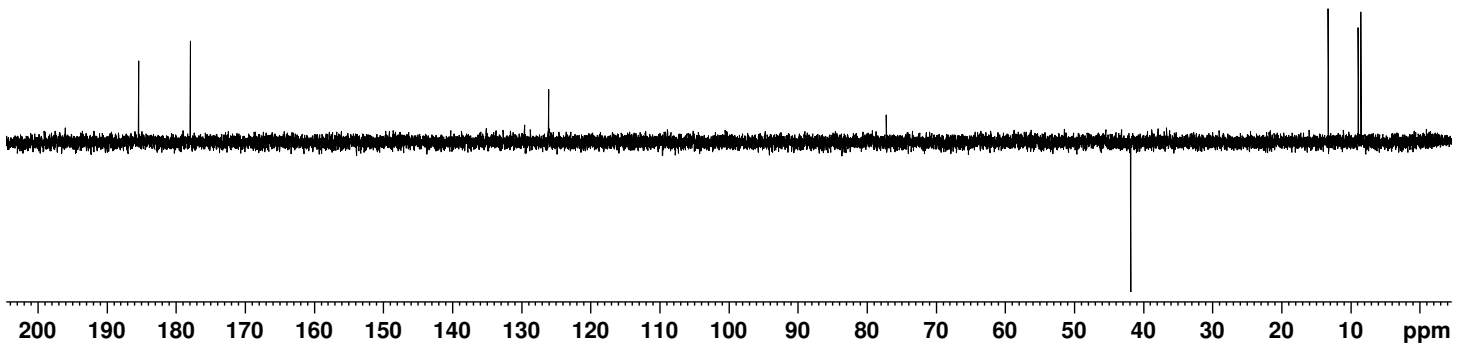


Figure S30. DEPT-135 NMR spectrum of **22b** in  $\text{DMSO}-d_6$ .

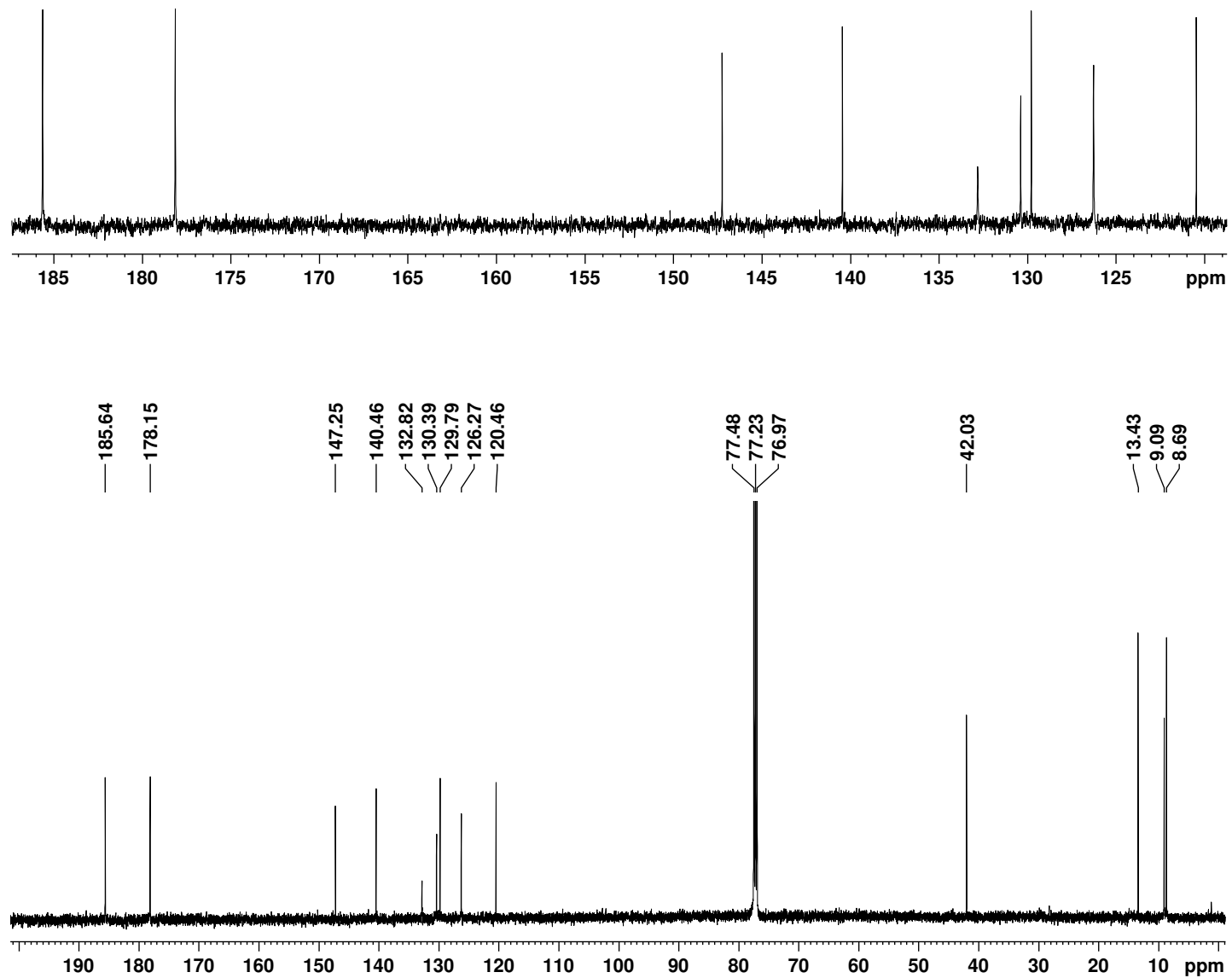


Figure S31.  $^{13}\text{C}$  NMR spectrum of **22b** in  $\text{DMSO}-d_6$ .

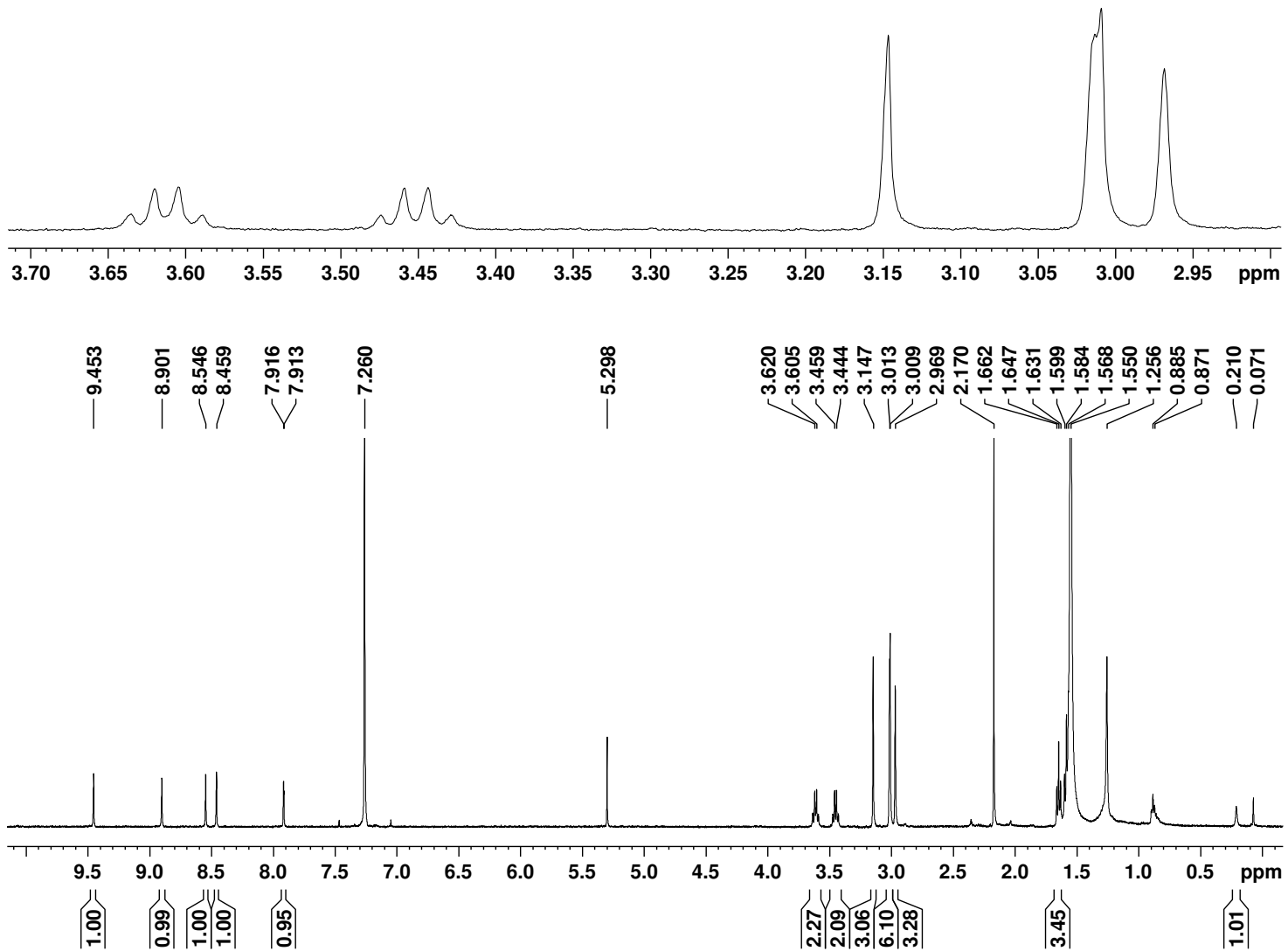


Figure S32. 500 MHz proton NMR spectrum of bromo-neo-confused porphyrin **8b** in  $\text{CDCl}_3$ .

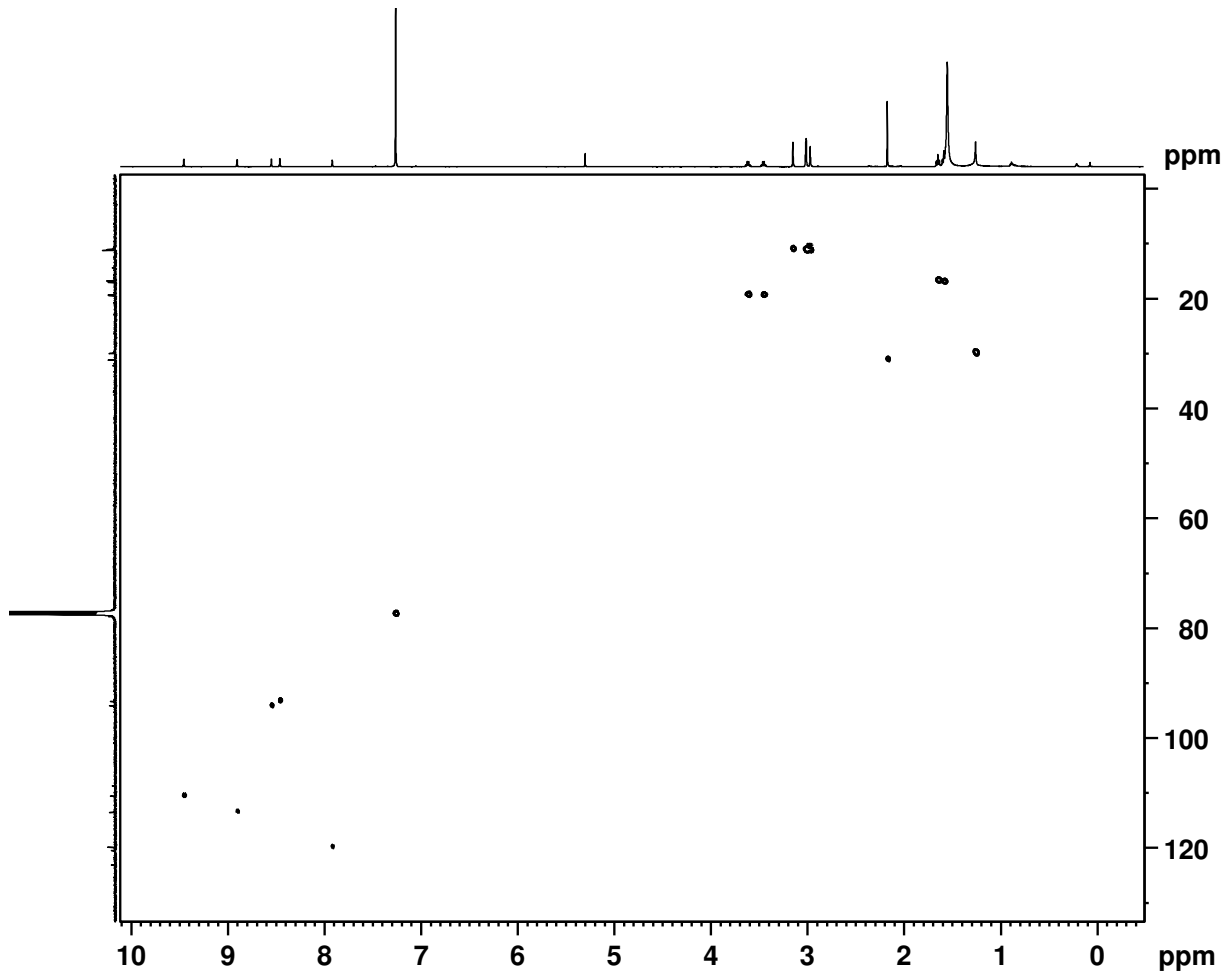


Figure S33. HSQC NMR spectrum of **8b** in  $\text{CDCl}_3$ .

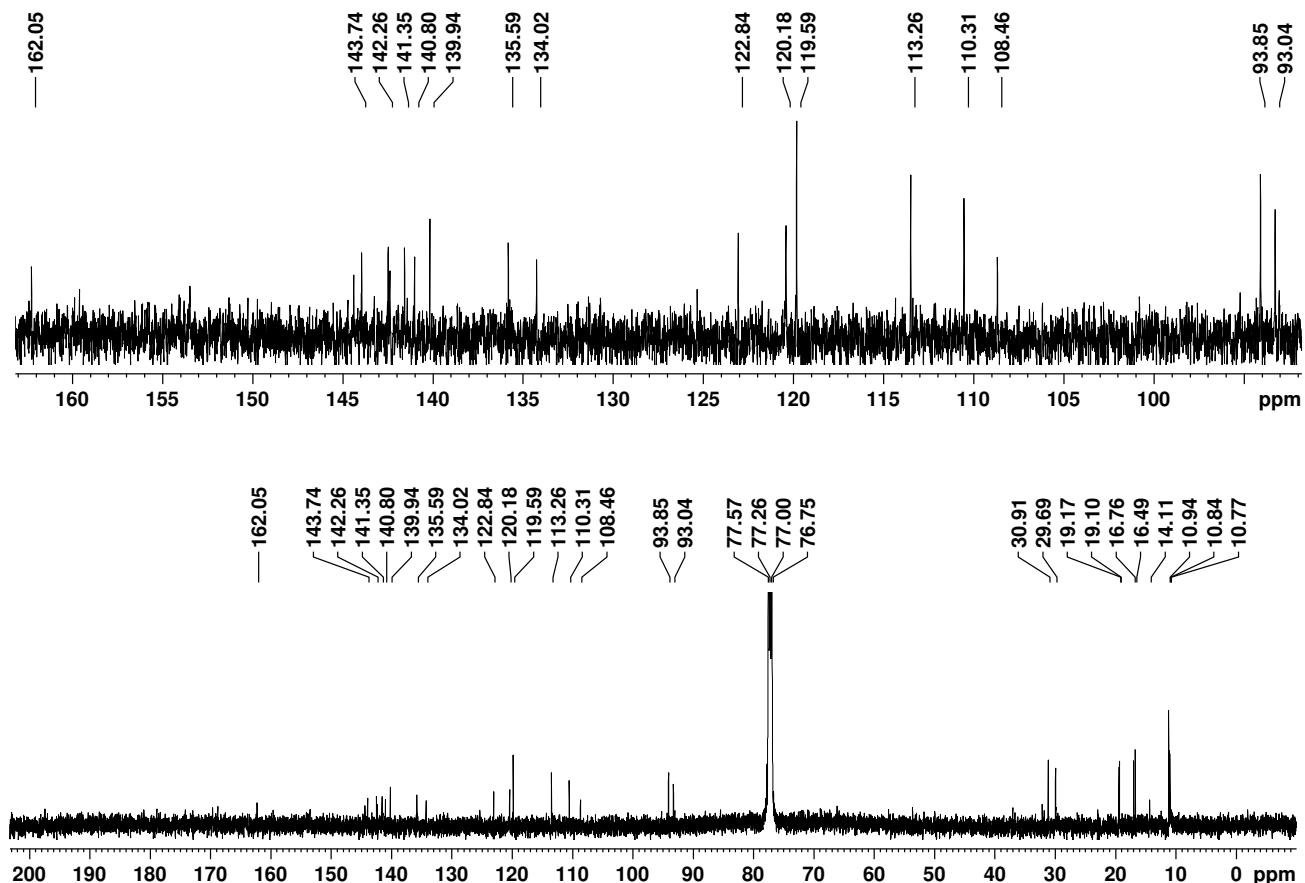


Figure S34. 125 MHz carbon-13 NMR spectrum of neo-confused porphyrin **8b** in CDCl<sub>3</sub>.

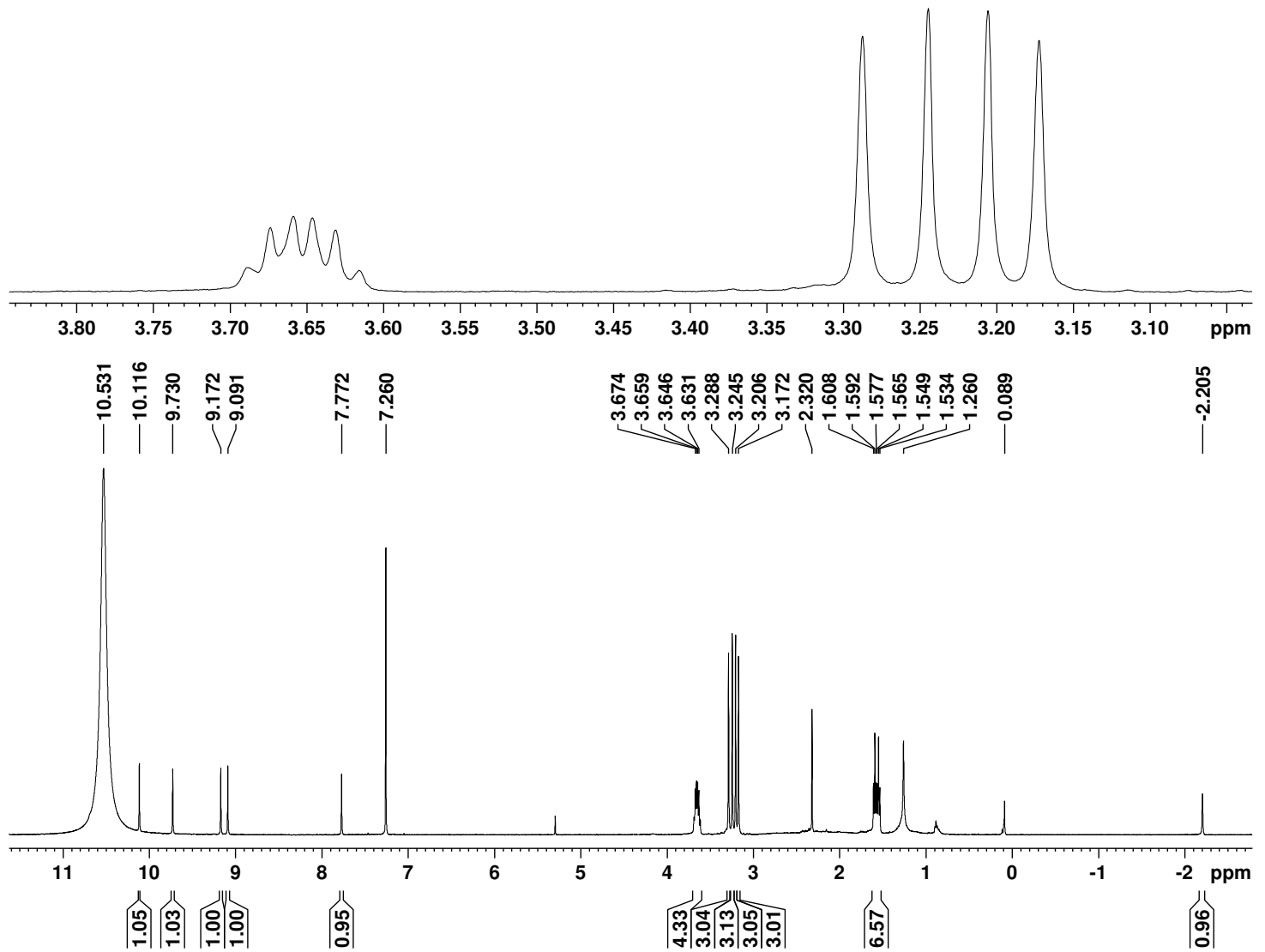


Figure S35. 500 MHz proton NMR spectrum of **8bH<sub>2</sub><sup>2+</sup>** in TFA-CDCl<sub>3</sub>.

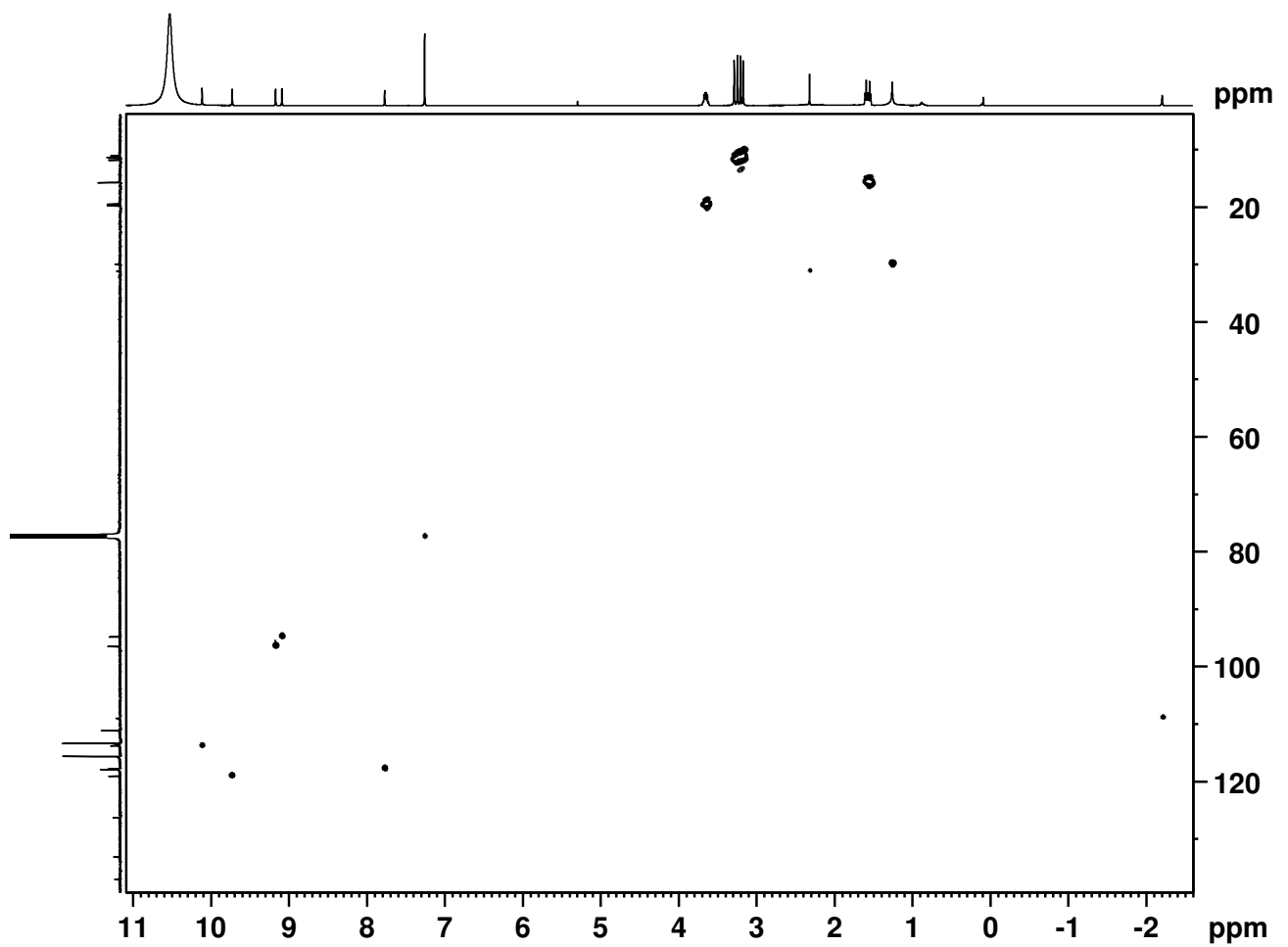


Figure S36. HSQC NMR spectrum of **8bH<sub>2</sub><sup>2+</sup>** in TFA-CDCl<sub>3</sub>.

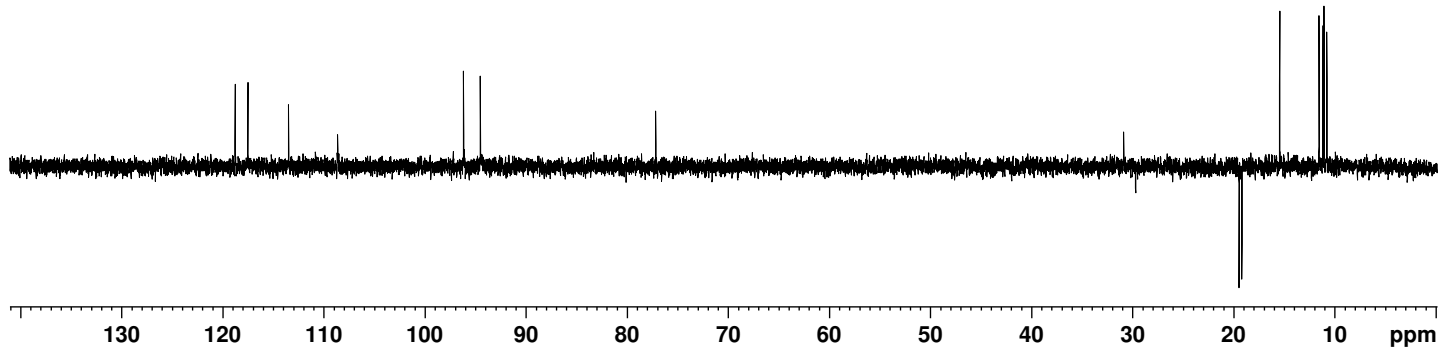


Figure S37. DEPT-135 NMR spectrum of **8bH<sub>2</sub>**<sup>2+</sup> in TFA-CDCl<sub>3</sub>.

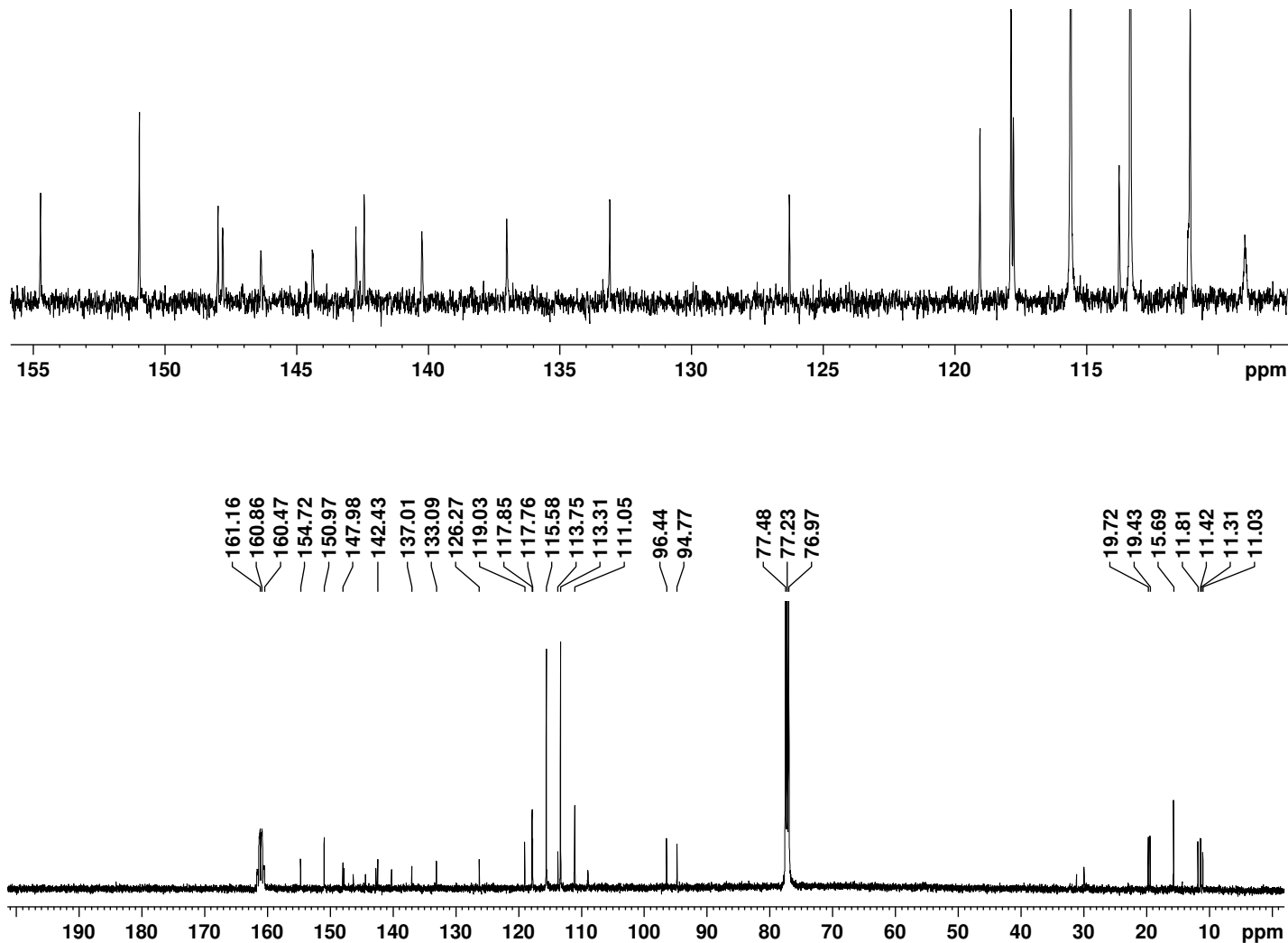


Figure S38. 125 MHz carbon-13 NMR spectrum of **8bH<sub>2</sub>**<sup>2+</sup> in TFA-CDCl<sub>3</sub>.

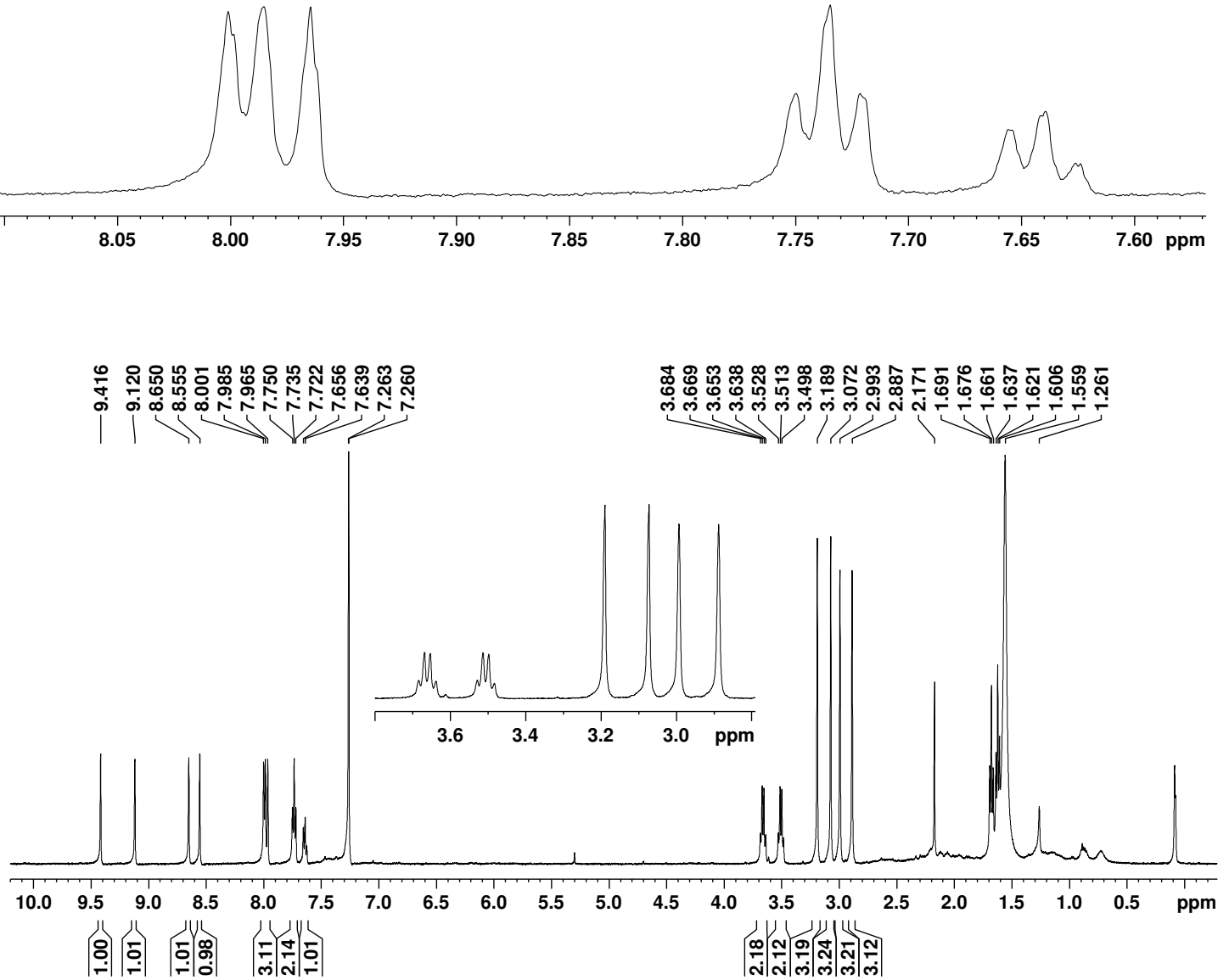


Figure S39. 500 MHz proton NMR spectrum of 3-phenyl-neo-confused porphyrin **8c** in  $\text{CDCl}_3$ .

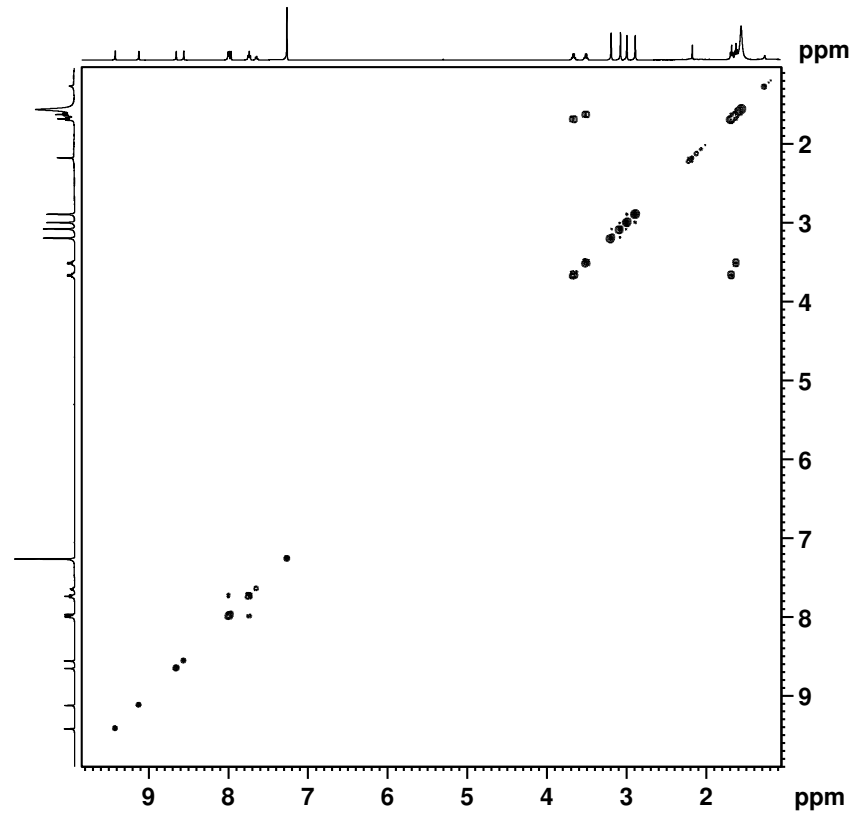


Figure S40. <sup>1</sup>H-<sup>1</sup>H COSY NMR spectrum of **8c** in  $\text{CDCl}_3$ .

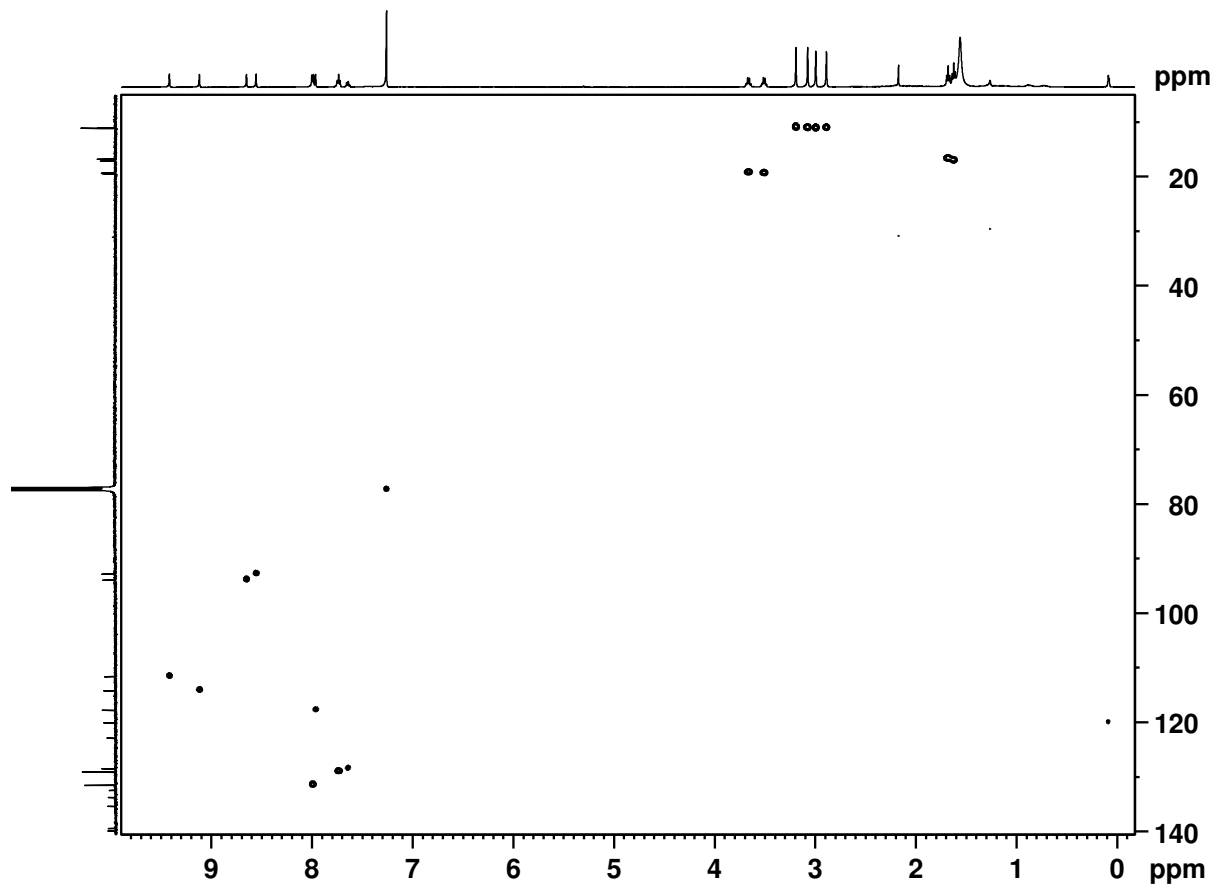


Figure S41. HSQC NMR spectrum of **8c** in  $\text{CDCl}_3$ .

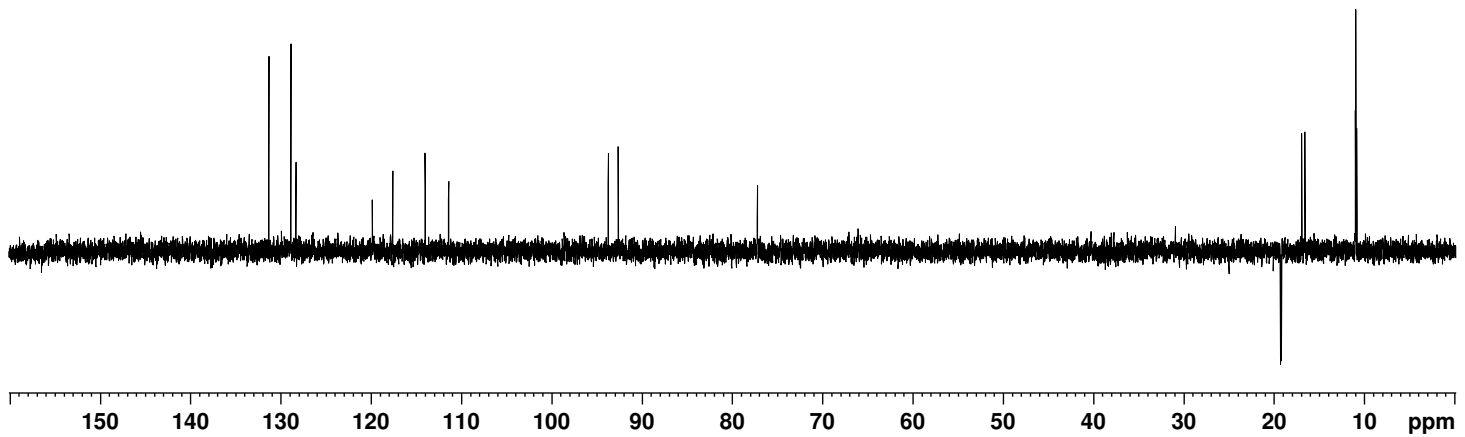


Figure S42. DEPT-135 NMR spectrum of **8c** in  $\text{CDCl}_3$ .

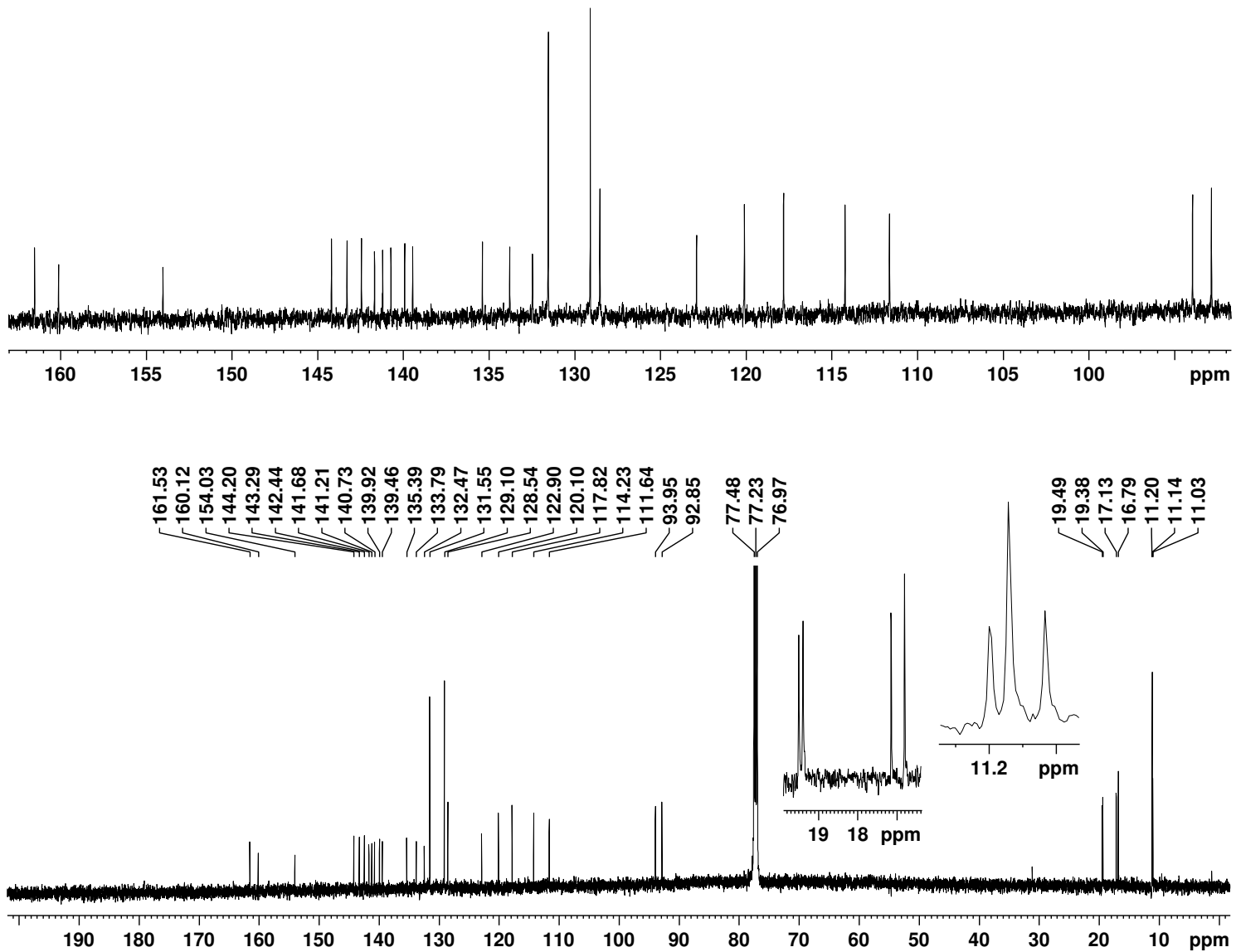


Figure S43.  $125\text{ MHz}$  carbon-13 NMR spectrum of **8c** in  $\text{CDCl}_3$ .

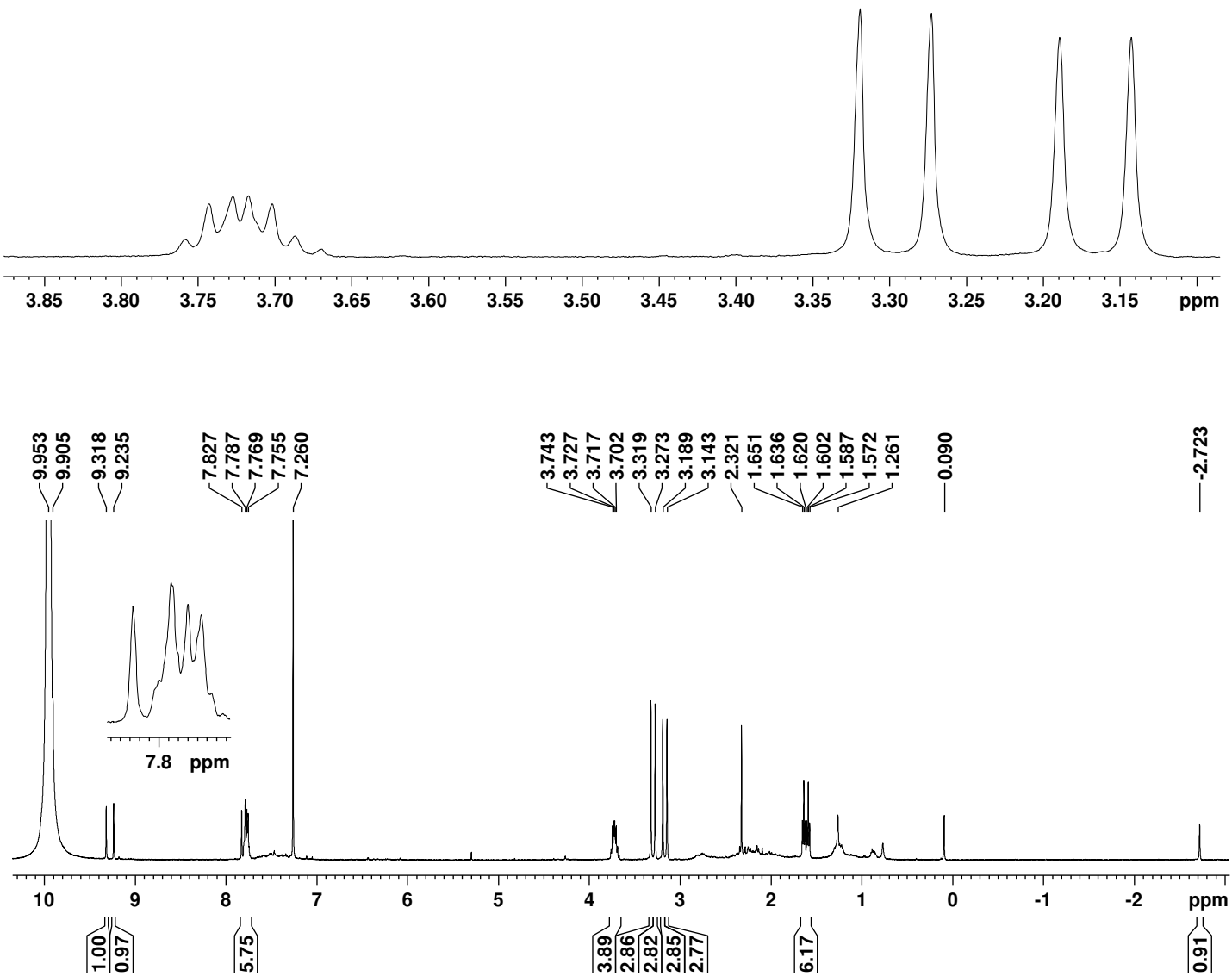


Figure S44. 500 MHz proton NMR spectrum of **8c**H<sub>2</sub><sup>2+</sup> in TFA-CDCl<sub>3</sub>.

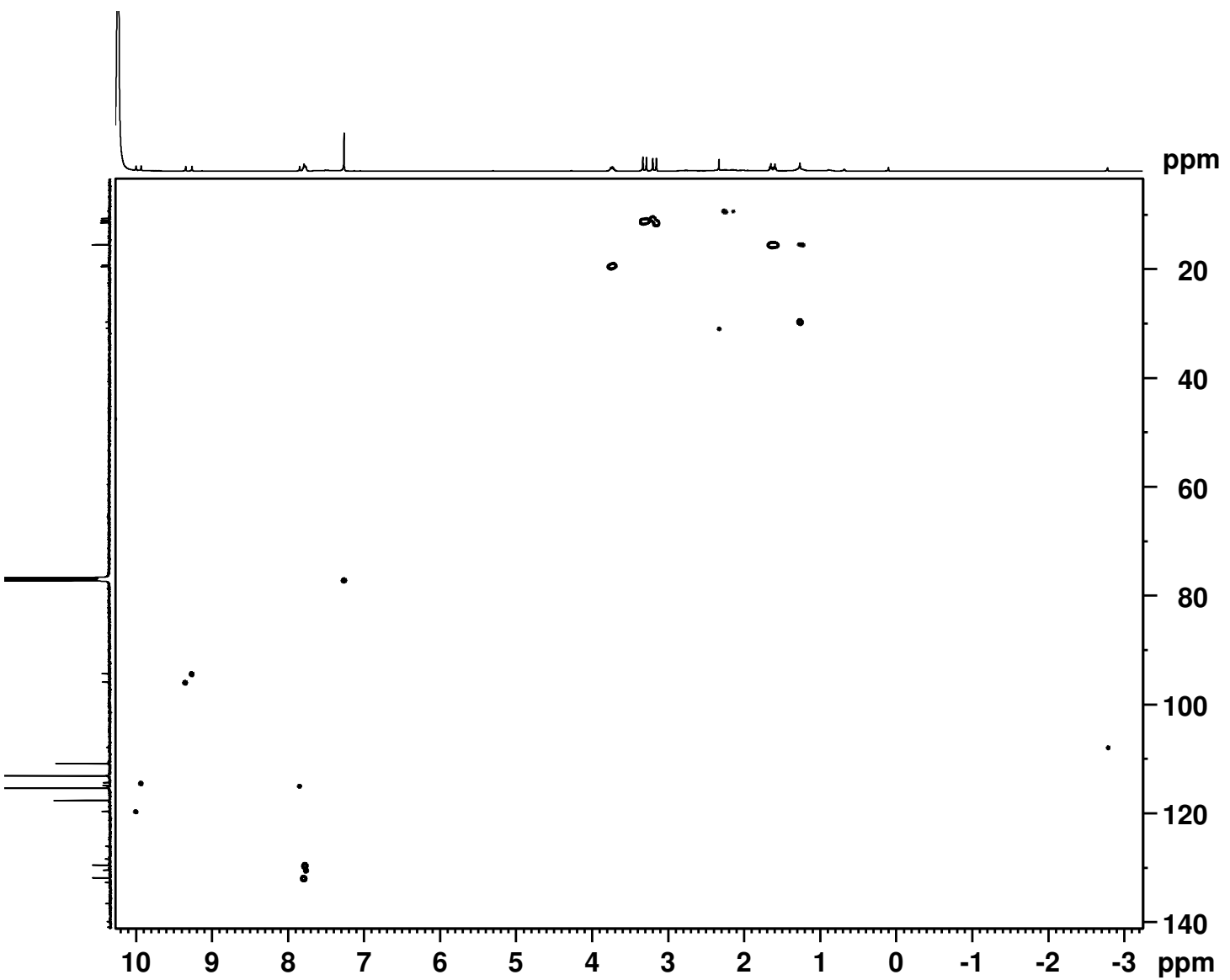


Figure S45. HSQC NMR spectrum of  $8\text{cH}_2^{2+}$  in TFA- $\text{CDCl}_3$ .

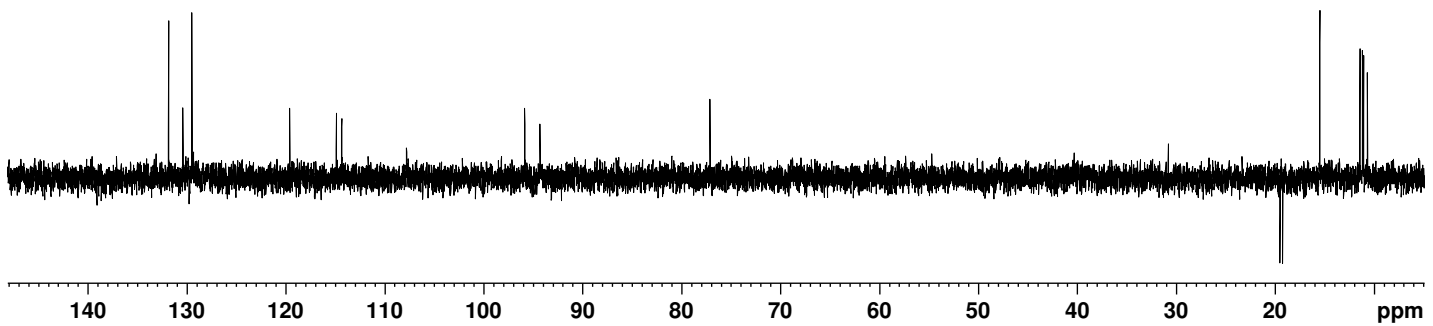


Figure S46. DEPT-135 NMR spectrum of **8c**H<sub>2</sub><sup>2+</sup> in TFA-CDCl<sub>3</sub>.

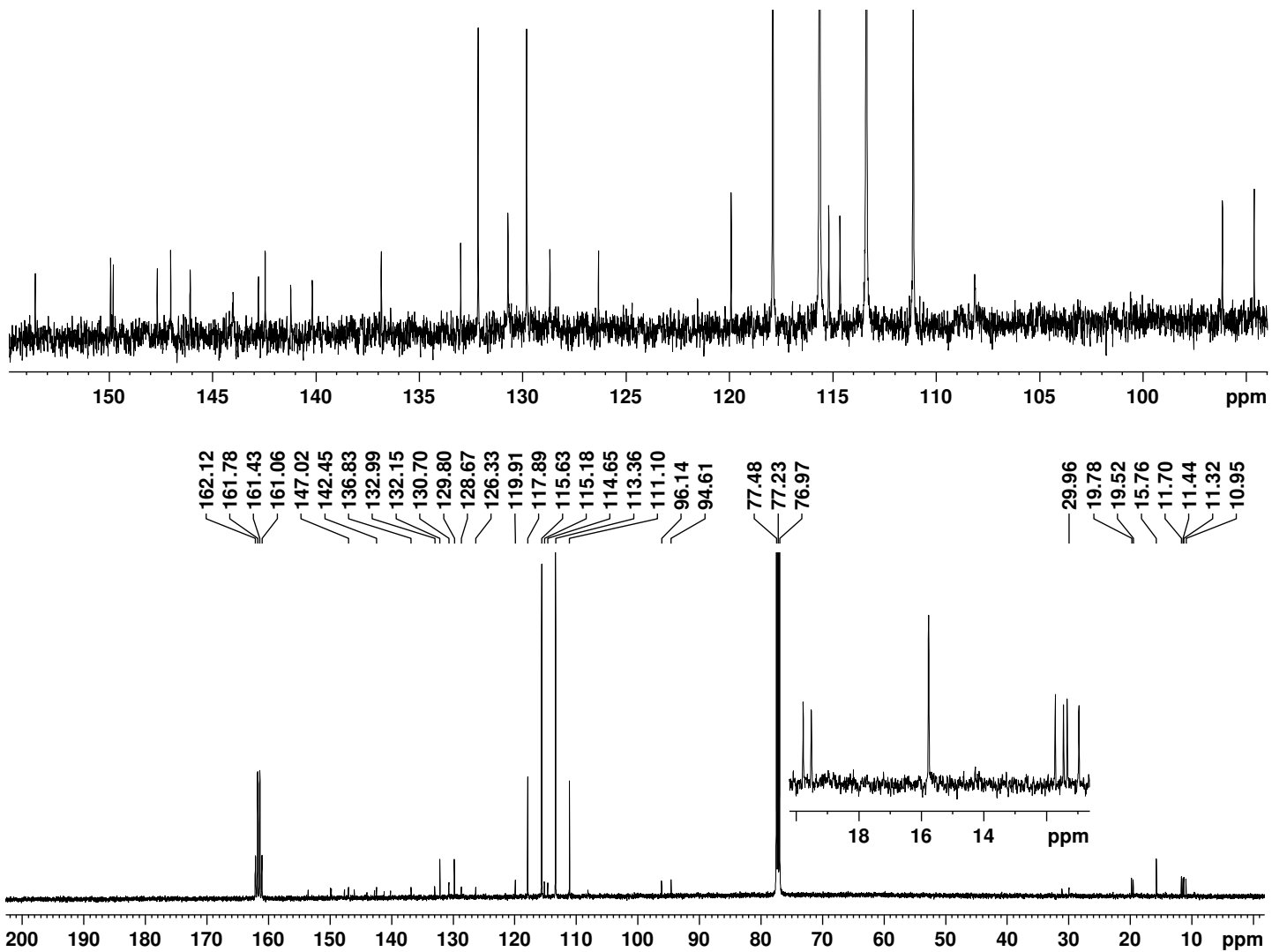


Figure S47. 125 MHz carbon-13 NMR spectrum of **8c**H<sub>2</sub><sup>2+</sup> in TFA-CDCl<sub>3</sub>.

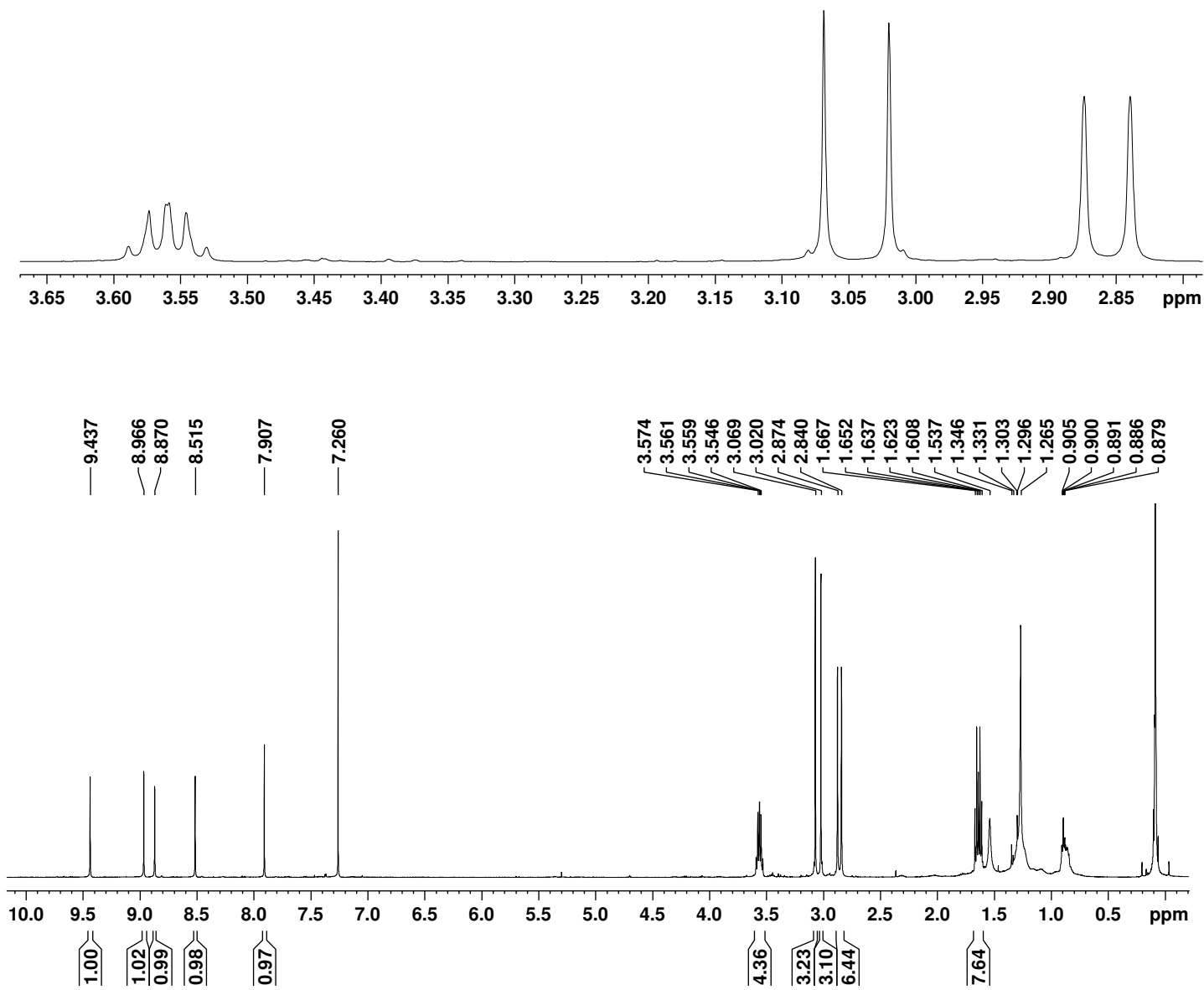


Figure S48. 500 MHz proton NMR spectrum of nickel(II) neo-confused porphyrin **18b** in  $\text{CDCl}_3$ .

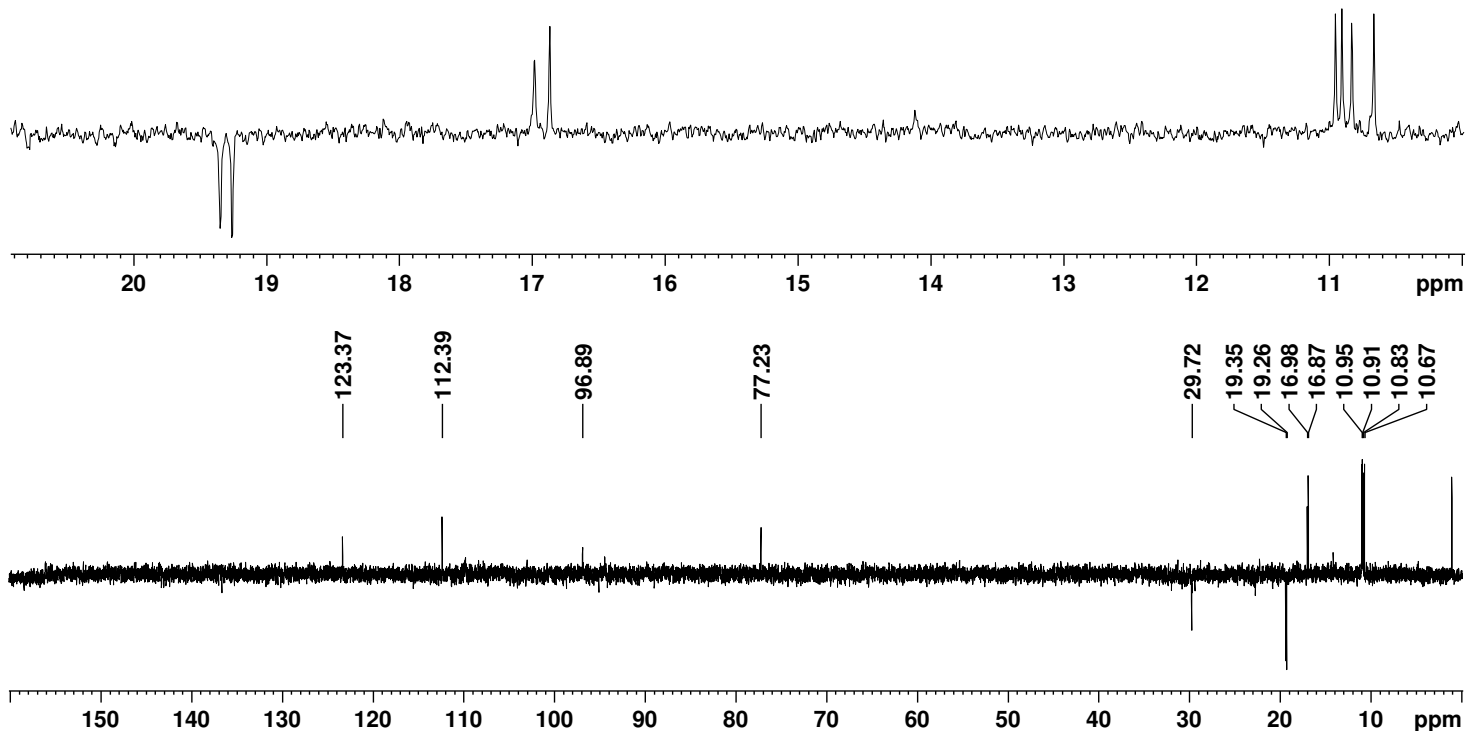


Figure S49. DEPT-135 NMR spectrum of **18b** in  $\text{CDCl}_3$ .

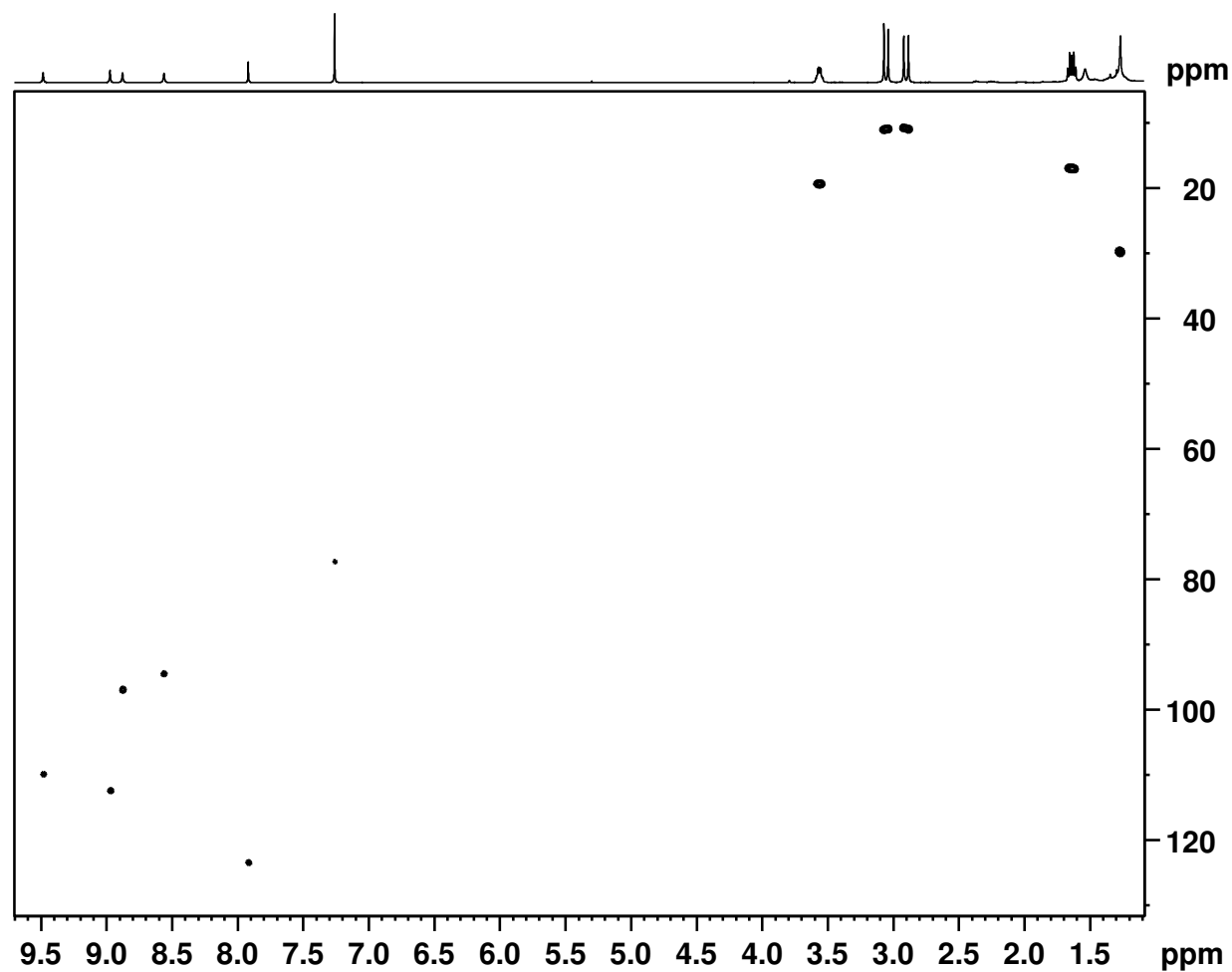


Figure S50. HSQC NMR spectrum of nickel complex **18b** in  $\text{CDCl}_3$ .

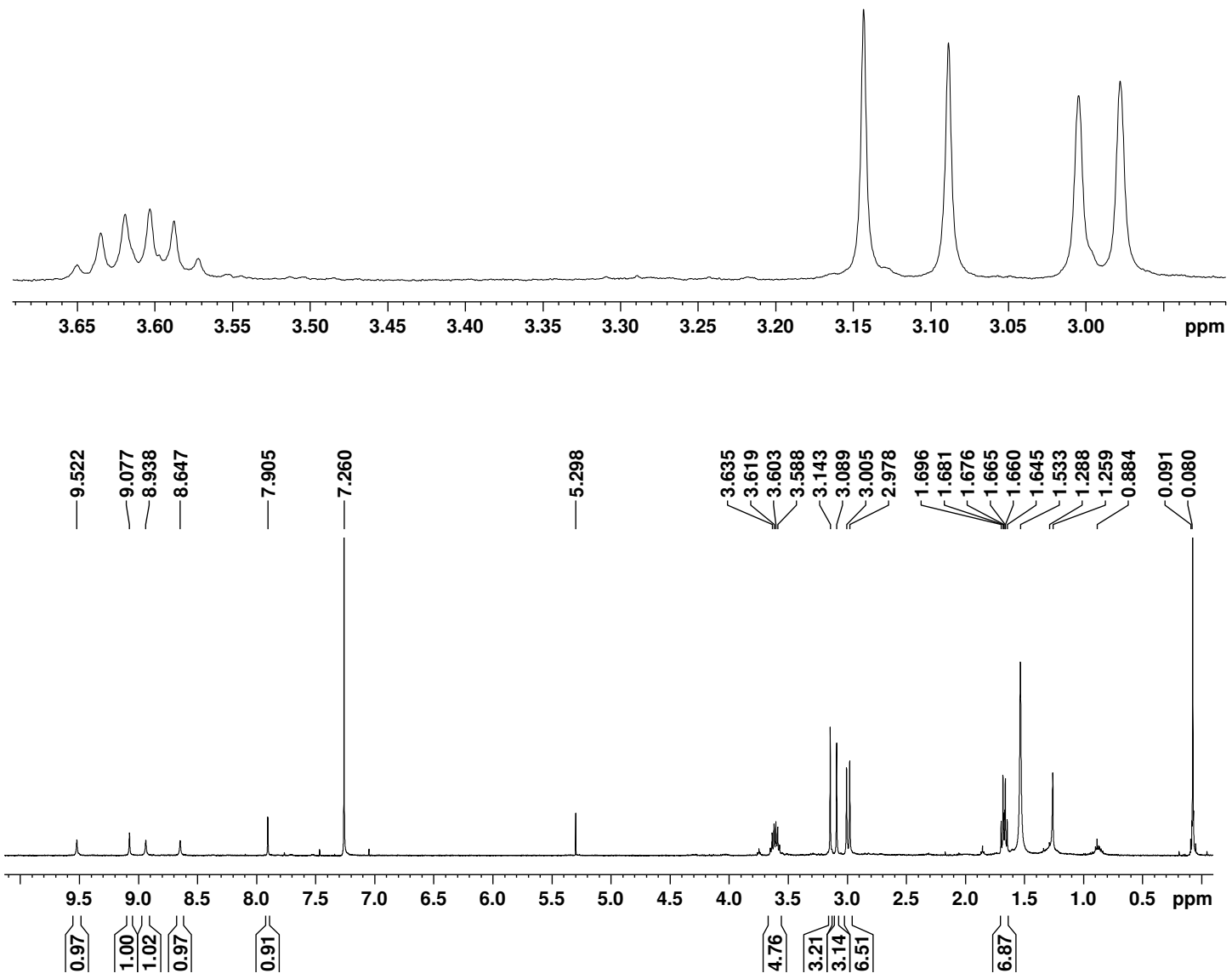


Figure S51. 500 MHz proton NMR spectrum of palladium(II) neo-confused porphyrin **19b** in  $\text{CDCl}_3$ .

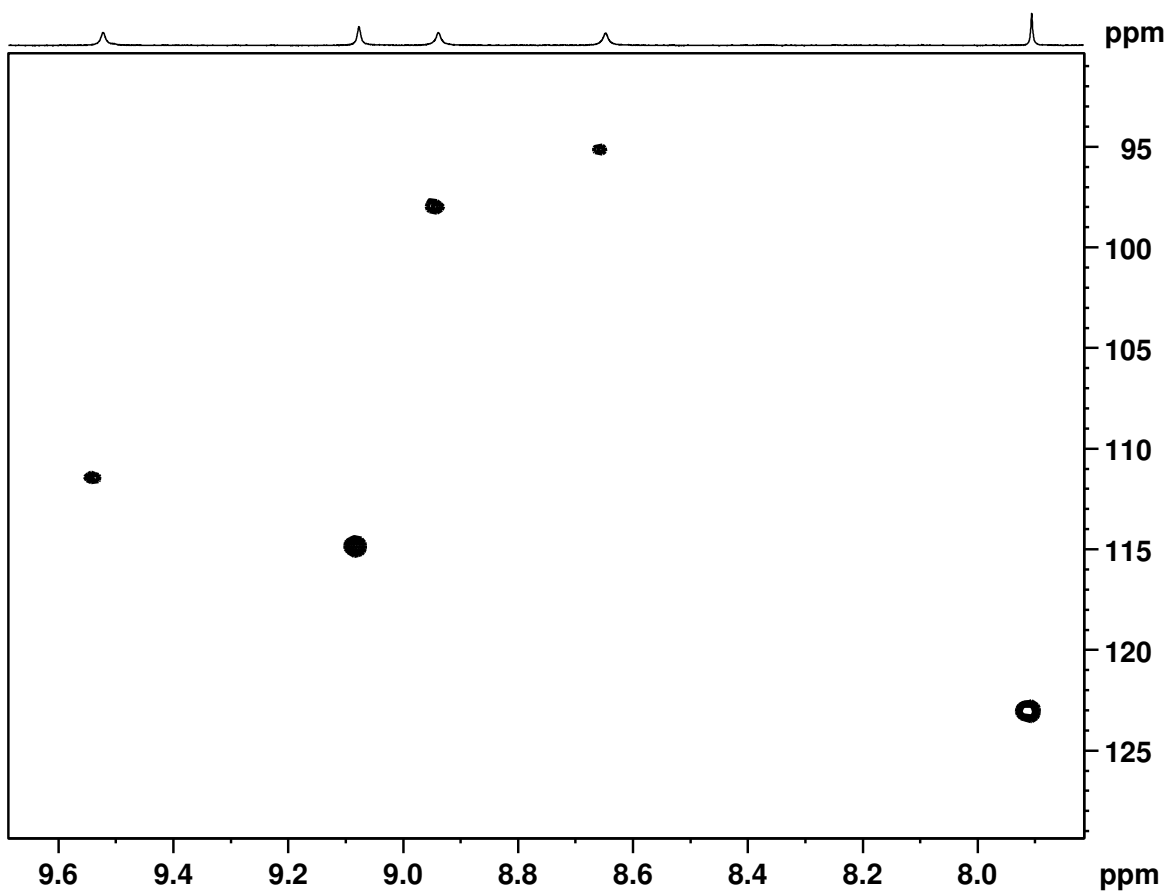
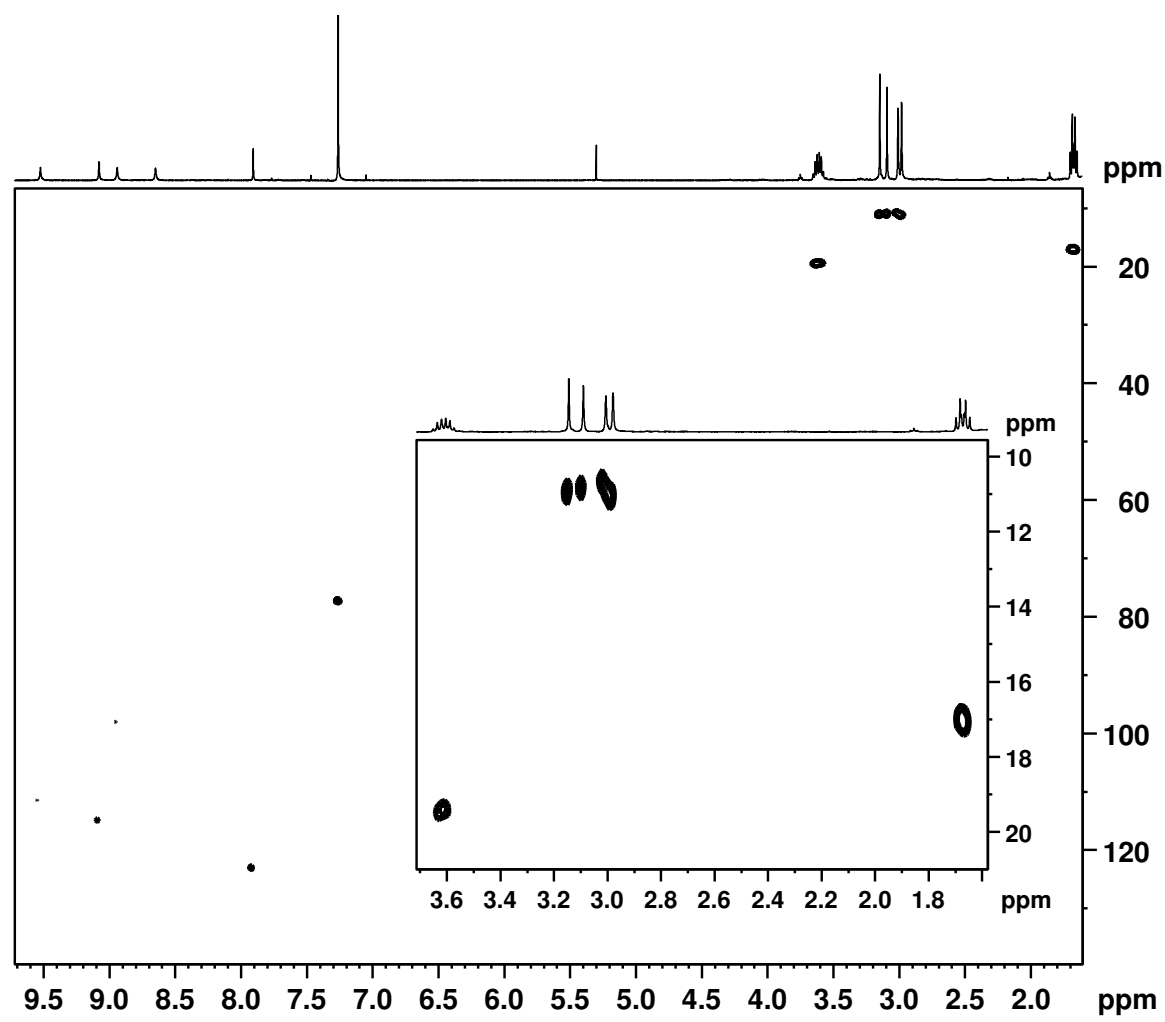


Figure S52. HSQC NMR spectrum of palladium(II) complex **19b** in  $\text{CDCl}_3$ .

TOF MS EI+  
9.23e5

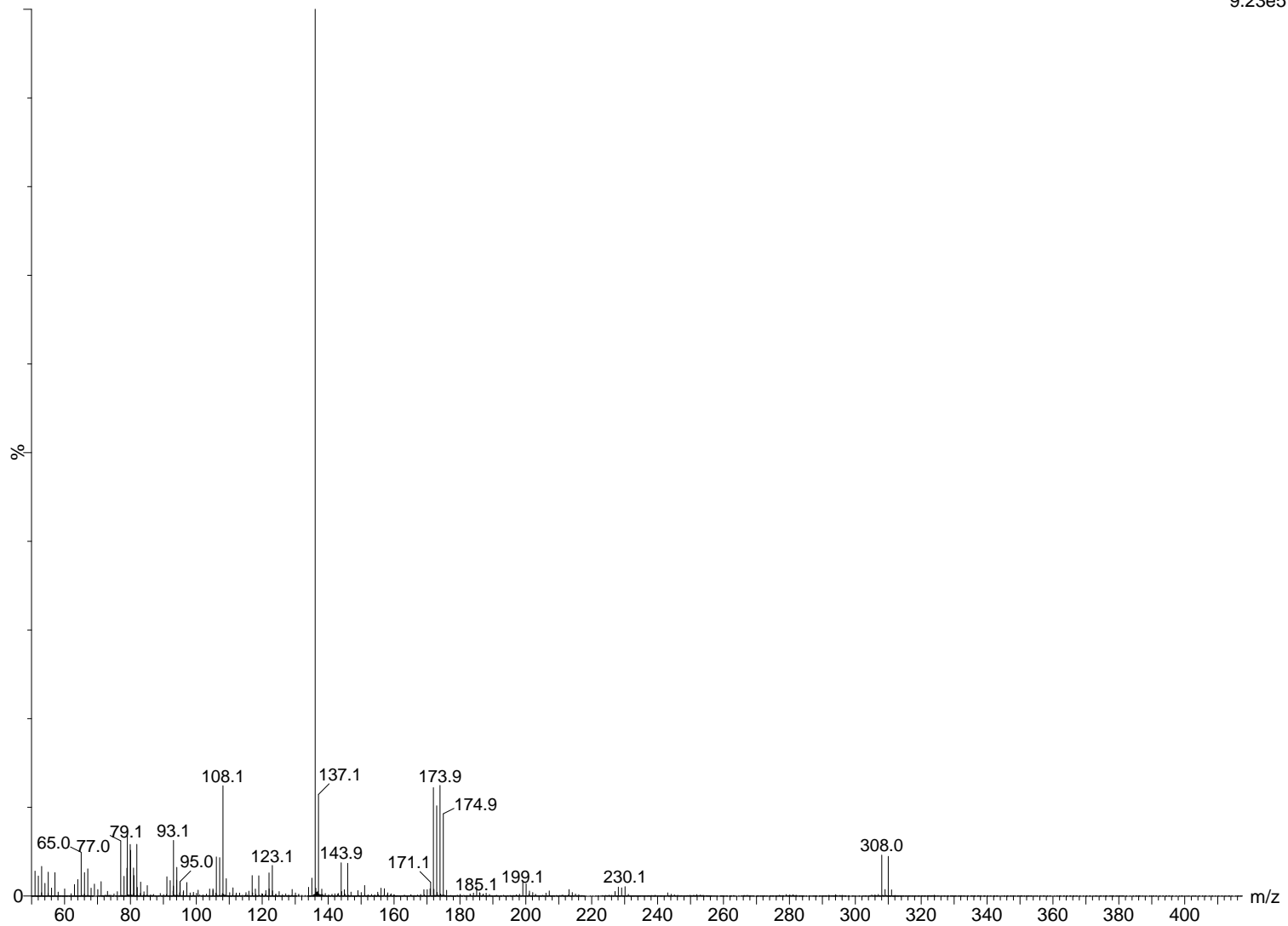


Figure S53. Electron-impact mass spectrum of bromo-1,2'-dipyrrylmethane **9b**.

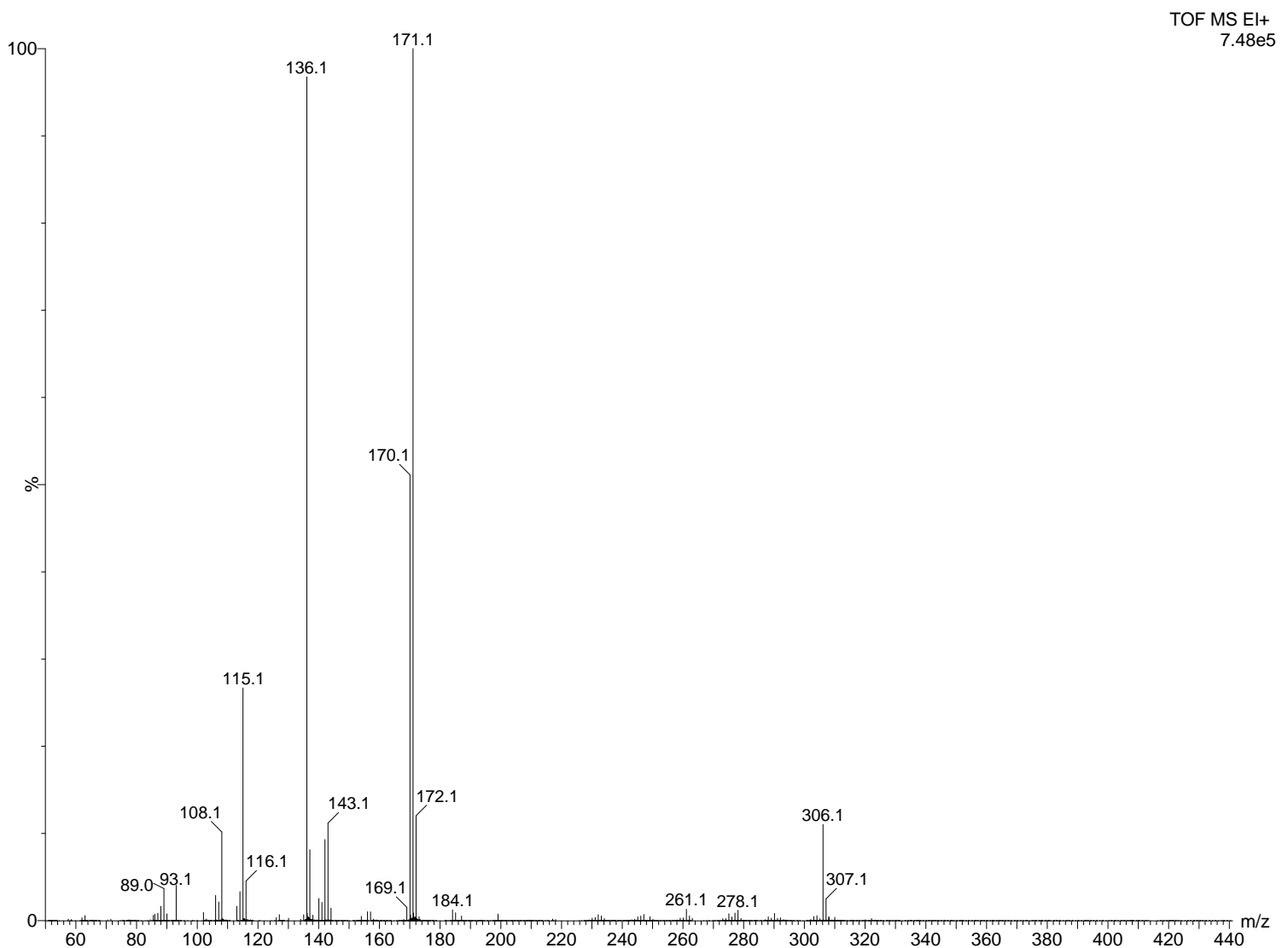


Figure S54. Electron-impact mass spectrum of phenyl-1,2'-dipyrrylmethane **9c**.

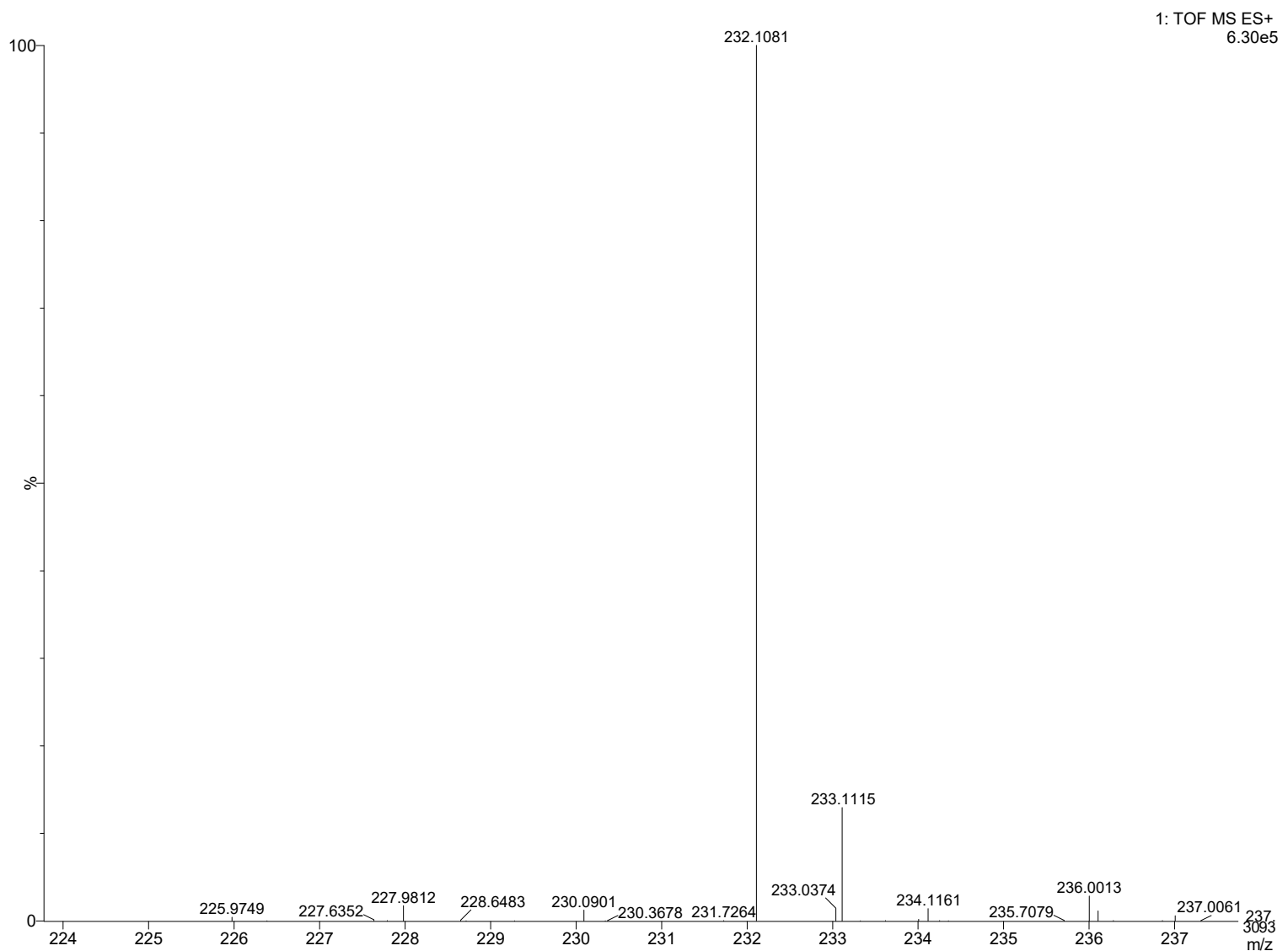


Figure S55. ESI mass spectrum of pyrrolylmethylimidazole **22a**.

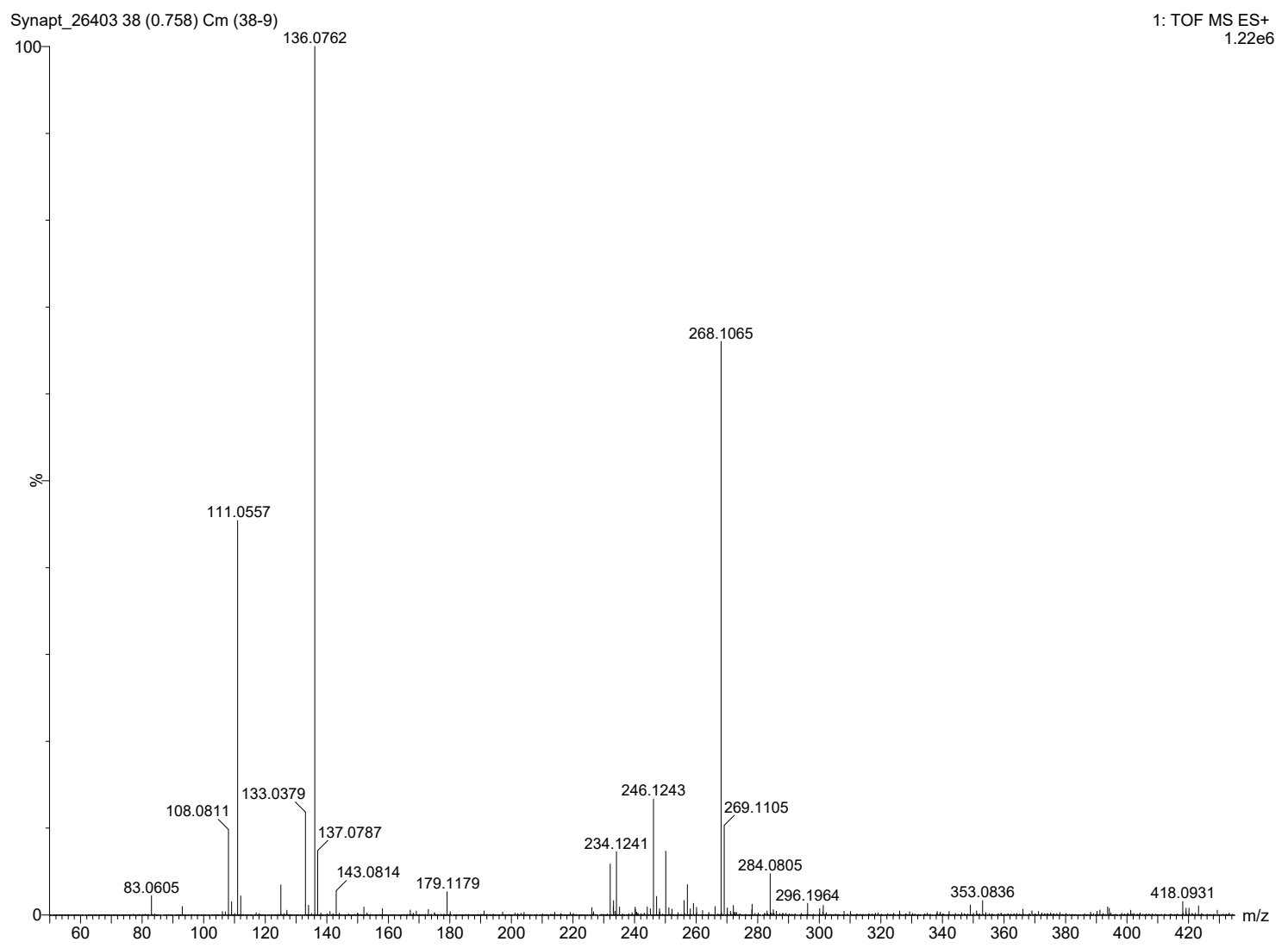


Figure S56. ESI MS of pyrrolylmethylimidazole **22b**.

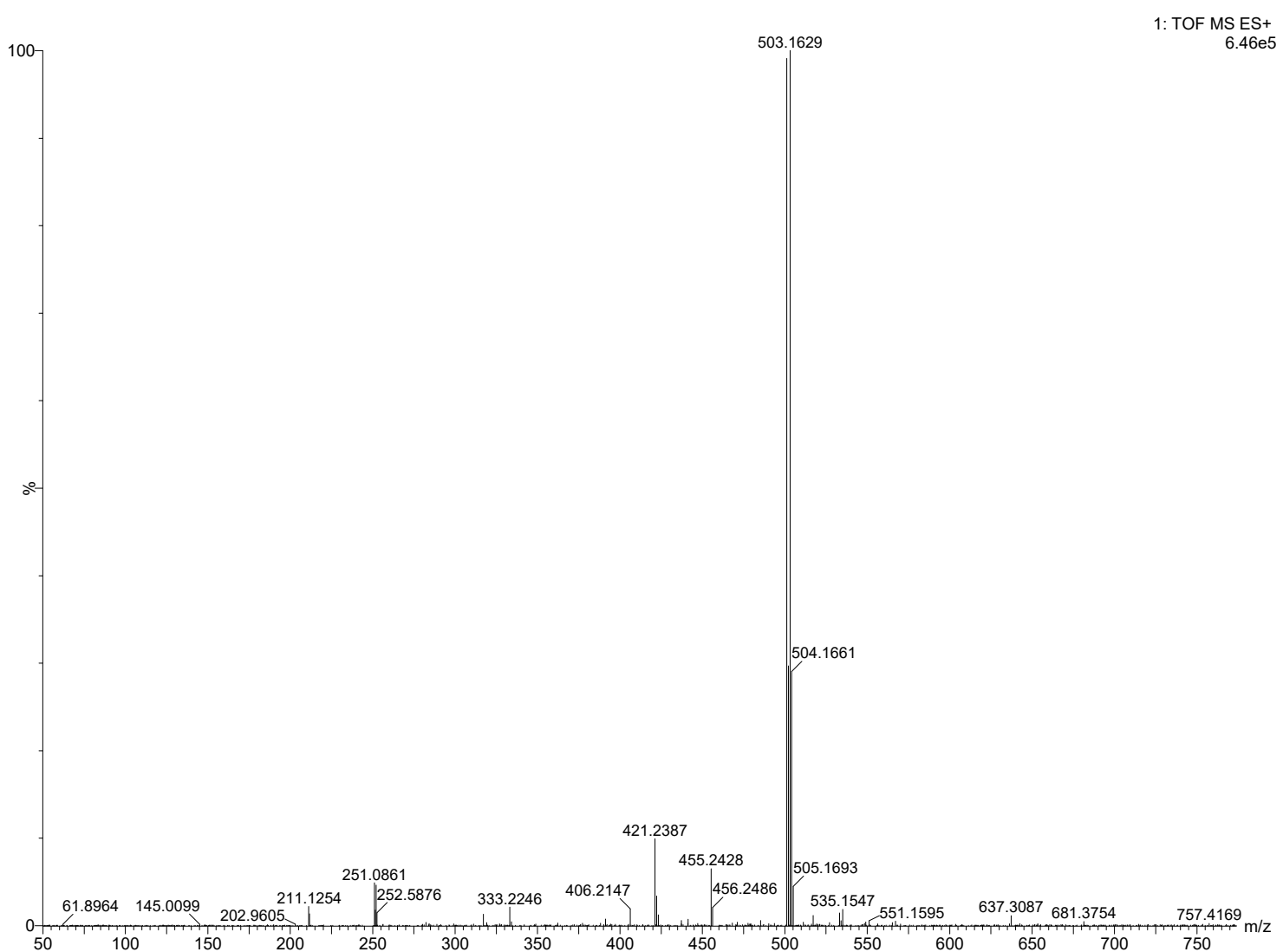


Figure S57. ESI MS of bromo-neo-confused porphyrin **8b**.

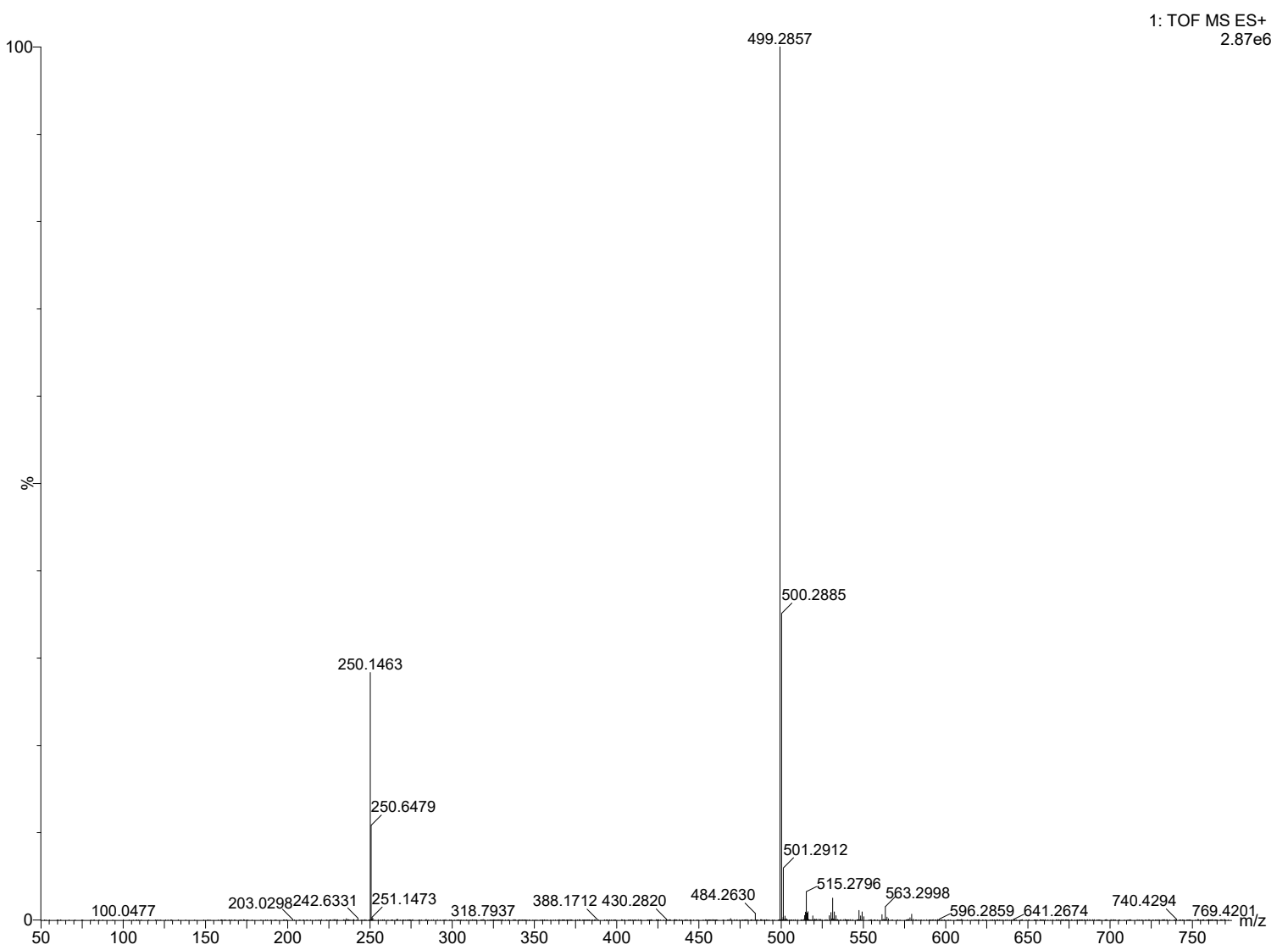


Figure S58. ESI MS of phenyl neo-confused porphyrin **8c**.

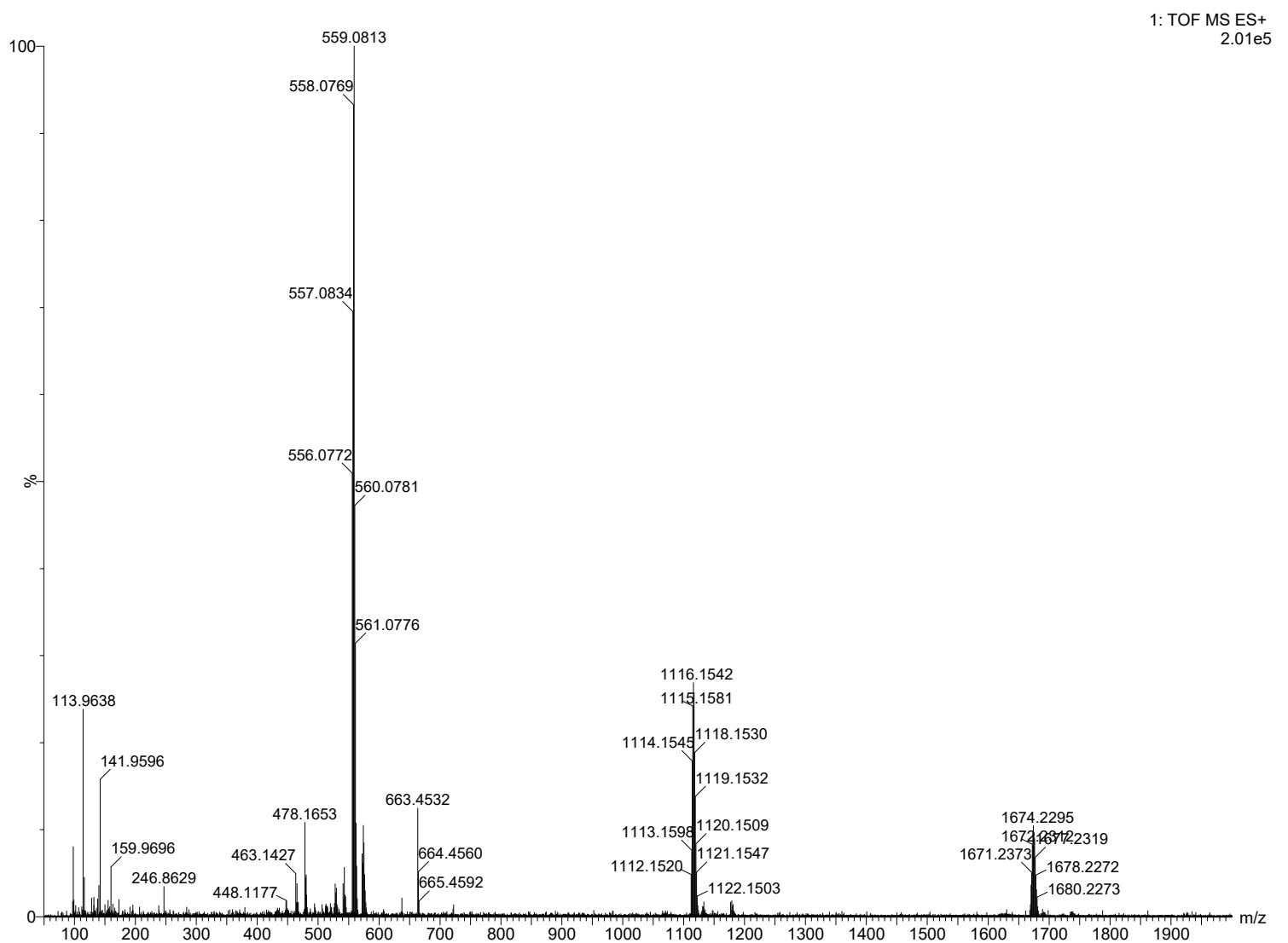


Figure S59. ESI MS of nickel complex **18b**.

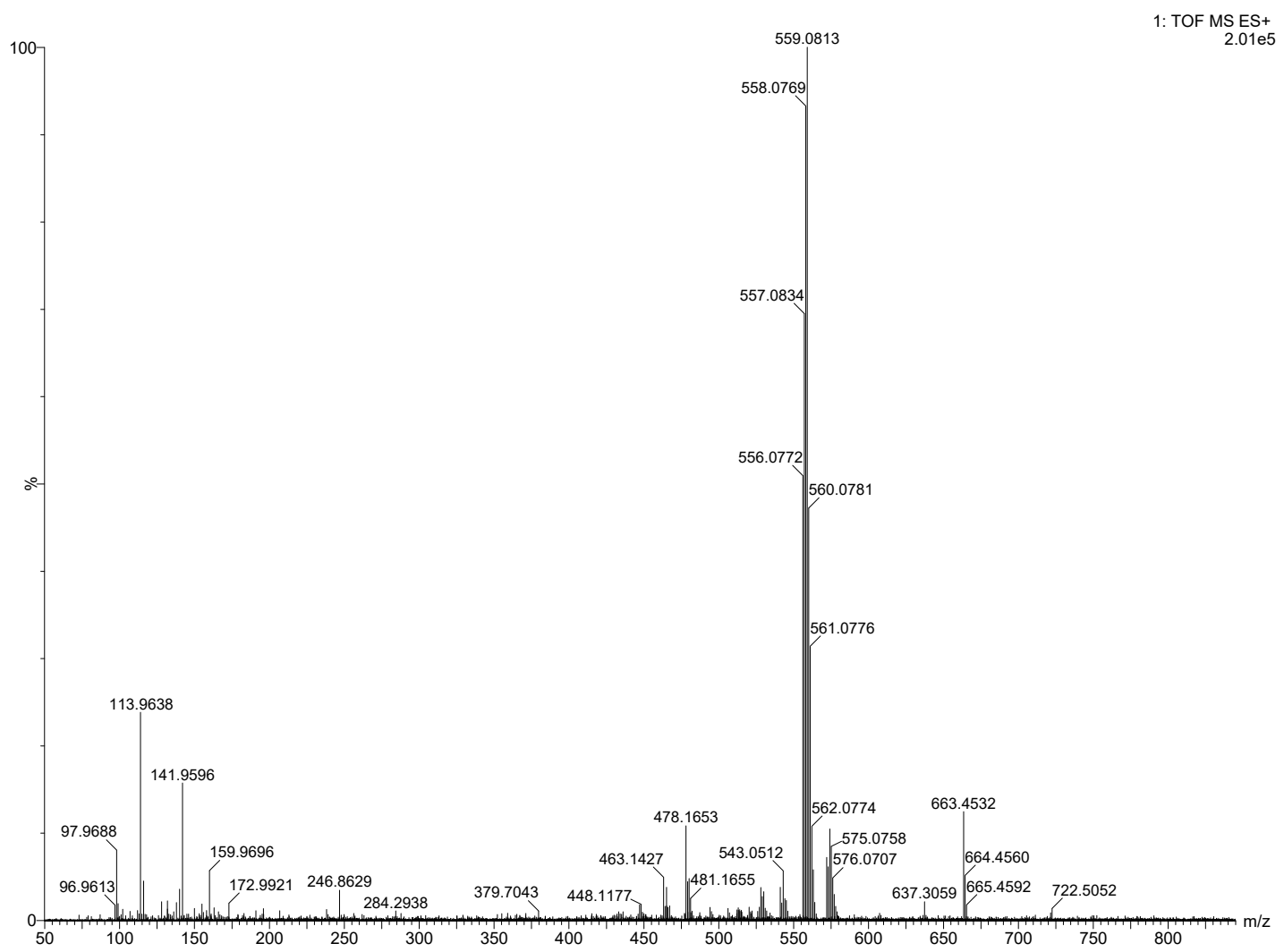


Figure S60. Details of the ESI MS for nickel complex **18b**.

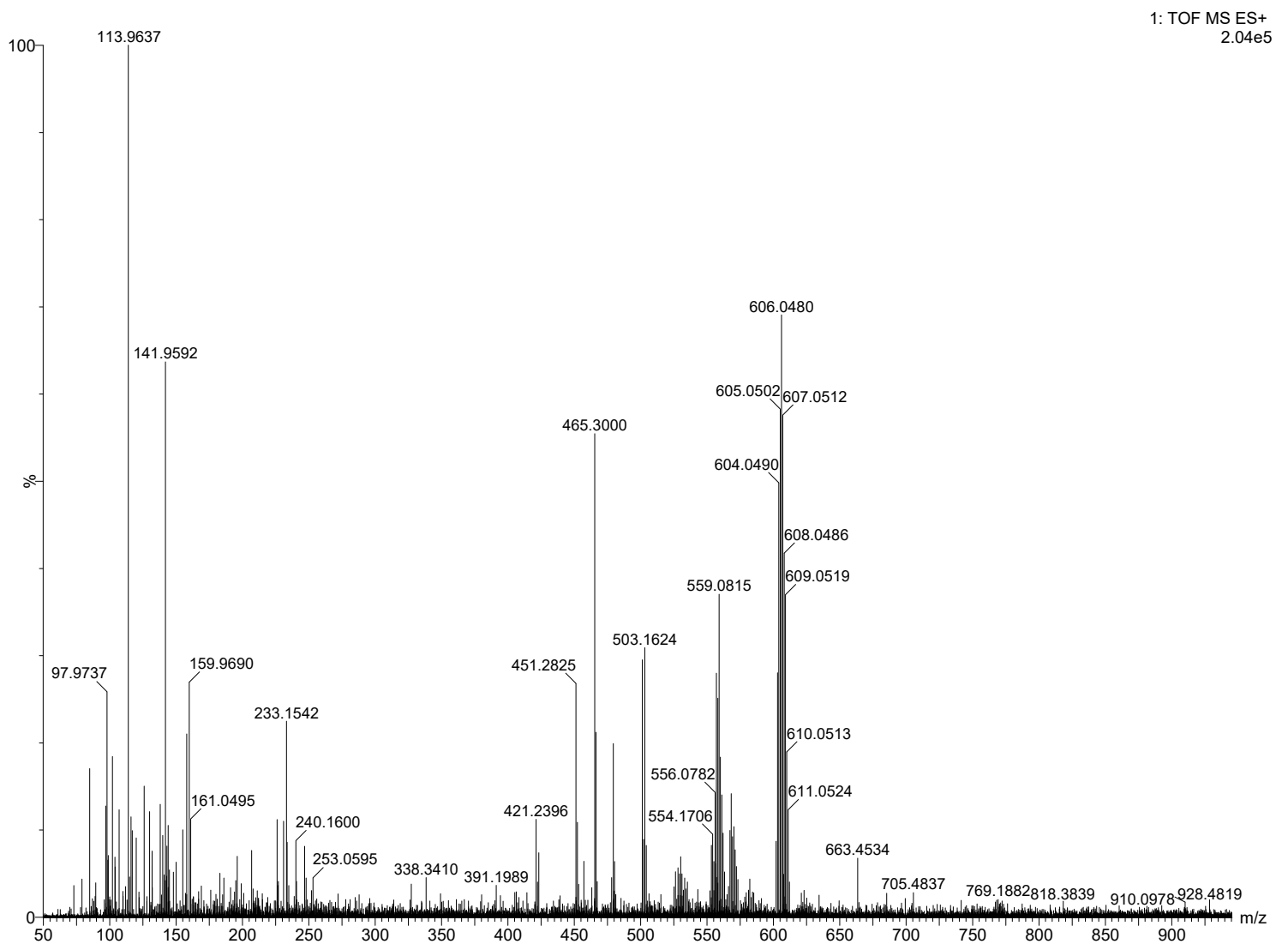


Figure S61. ESI MS of palladium(II) complex **19b**.